Annu. Rev. Astron. Astrophys. 2005. 43:625–76
doi: 10.1146/annurev.astro.41.011802.094927

First published online as a Review in Advance on June 14, 2005

MEGA-MASERS AND GALAXIES

K.Y. Lo
National Radio Astronomy Observatory, Charlottesville, Virgina 22903; Institute of Astronomy and Astrophysics, Academia Sinica, Taipei, Taiwan, R.O.C.; email: flo@nrao.edu

Key Words accretion disks, active galactic nuclei, maser emission, molecular clouds, star-bursts

■ **Abstract** In the Galaxy, microwave radiation can be amplified in the interstellar medium in the immediate neighborhood of young stellar objects, or circumstellar envelopes around evolved stars, resulting in cosmic maser emission. Cosmic masers exist because, in contrast to terrestrial conditions, the interstellar gas density is very low so that level population in molecules is typically not in thermal equilibrium, and sometimes inverted. In the nuclear regions of external galaxies, there exist very powerful OH (λ18 cm) and H_2O (λ1.35 cm) cosmic masers with line luminosities of $\sim 10^2$–$10^4\ L_\odot$, $\geq 10^6$ times more luminous than typical Galactic maser sources. These are the "mega-masers," found in high-density molecular gas located within parsecs of active galactic nuclei in the case of H_2O mega-masers, or within the central 100 pc of nuclear star-burst regions in the case of OH mega-masers. H_2O mega-masers are most frequently found in galactic nuclei with Seyfert2 or LINER spectral characteristics, in spiral and some elliptical galaxies. OH mega-masers are found in ultra-luminous IR galaxies (ULIRG) with the warmest IR colors, and importantly, the OH luminosity is observed to increase with the IR luminosity: $L_{OH} \propto L_{IR}^{1.2}$. Because of the extremely high-surface brightness, H_2O mega-maser emission can be mapped at sub-milli-arc-second resolution by Very Long Baseline Interferometry (VLBI), providing a powerful tool to probe spatial and kinematic distributions of molecular gas in distant galactic nuclei at scales below one parsec. An excellent example is the active galaxy, NGC 4258, in which mapping of the H_2O mega-maser emission has provided the first direct evidence in an active galactic nucleus for the existence of a thin Keplerian accretion disk with turbulence, as well as highly compelling evidence for the existence of a massive black hole. The NGC 4258 mega-maser has also provided a geometric distance determination of extremely high precision. H_2O mega-maser emission is also found to arise from postshocked gas from the impact of nuclear jets or outflows on the surrounding molecular clouds. High-resolution observations have shown that OH mega-masers originate from the molecular gas medium in 100-pc scale nuclear star-burst regions. It is proposed that such extreme star-burst regions, with extensive high-density gas bathed in a very high far-IR radiation field, are conducive to the formation of a very large number of OH maser sources that collectively produce the OH mega-maser emission. In the early Universe, galaxies or mergers could go through a very luminous phase, powered by intensive star-bursts and AGN formation, and could have extremely large OH and H_2O maser luminosities, possibly producing giga-masers. With the increasing sensitivity

of new telescopes and receivers, surveys and high-resolution studies of mega-masers and giga-masers will be very important tracers and high-resolution probes of active galactic nuclei, dust embedded star-bursts in the earliest galaxies and galaxy mergers in the epoch of very active star formation at $z \sim 2$ and beyond. Distance determination of giga-masers at $z \sim 1$–2 can provide on independent measure of how fast the universe is expanding.

1. INTRODUCTION

The term "maser," an acronym for microwave amplification by stimulated emission of radiation, was given to the general type of devices first invented in the laboratory for the purposes of stable oscillator and high-resolution spectrometer (Gordon, Zeiger & Townes 1955). Masers do not occur naturally in laboratory environments where thermal equilibrium is the common condition. Under thermal equilibrium, radiation is generally absorbed by the medium it is propagating in, attenuated instead of being amplified. This is clear from considering the absorption coefficient of radiation in a medium:

$$\alpha_\nu = \frac{h\nu}{4\pi}\phi(\nu) n_{\rm l} B_{\rm lu}\left(1 - \frac{n_{\rm u}/g_{\rm u}}{n_{\rm l}/g_{\rm l}}\right),$$

where n and g are the number densities and statistical weights, respectively, of the upper and lower energy levels, u and l, hν is the energy of the radiative transition between the two levels, $B_{\rm lu}$ is the Einstein coefficient for absorption and $\phi(\nu)$ is the line profile function. Under thermal equilibrium,

$$\frac{n_{\rm u}/g_{\rm u}}{n_{\rm l}/g_{\rm l}} = \exp\left(-\frac{h\nu}{kT}\right) < 1,$$

and α_ν is positive, meaning that the radiation is absorbed as it propagates in the medium at temperature T.

In the interstellar medium, maser[1] emission occurs naturally, originating typically in high density ($n(\mathrm{H_2}) \geq 10^7$ cm^{-3}, which on the other hand is extremely low compared to terrestrial conditions) gas near an excitation source or a source of energy. This is because in the vast volume outside of stars the conditions are typically out of thermal equilibrium. Under such conditions, where the gas density is below the critical density for collisional de-excitation, excited atoms or molecules decay radiatively and can end up with a population inversion, which means that $\frac{n_{\rm u}/g_{\rm u}}{n_{\rm l}/g_{\rm l}} > 1$. In this case, $\alpha_\nu < 0$ so that the radiation is amplified as it propagates through the medium. Furthermore, in the astronomical context, the path length, L, is large enough (AU to pc scale) that the amplification factor $\exp(-\int \alpha_\nu \mathrm{d}L)$ is

[1]In the astronomical context, the term maser is used to denote the process of amplification by stimulated emission.

significant. For these reasons, cosmic masers are not uncommon natural phenomena in the cosmos.[2]

Cosmic OH and H_2O masers (emitting at $\lambda = 18$ cm and 1.35 cm respectively, or $\nu = 1.6$ GHz and 22.2 GHz) are two of the most common found in the Galaxy. They were discovered serendipitously because of their unexpectedly large flux density (Gundermann 1965, Weaver et al. 1965, Cheung et al. 1969). At the radio wavelengths involved, where $hc/\lambda kT \ll 1$ (the Rayleigh-Jeans limit), it is convenient to measure the observed flux density S_ν per unit solid angle (surface brightness), or intensity, by the brightness temperature $T_b \equiv S_\nu/\Omega_s \times \lambda^2/2k$, where Ω_s is the solid angle of the emission region. If the emission is thermal in origin, T_b equals T, the physical temperature of the source (or the temperature times the optical depth if the source is optically thin.) In the case of non-thermal radiation, T_b can be much larger than T, ranging up to 10^{14} K. Thus, T_b provides important information about the source of emission directly. In practice, T_b can be determined only when the source size Ω_s is known. For example, the OH maser source size was finally resolved after a series of efforts of building interferometers of increasingly longer baselines (B) and therefore increasingly higher angular resolution (λ/B), until Very Long Baseline Interferometry (VLBI) with baselines of thousands of kilometers and milli-arc-second (mas) resolution was achieved (Clark et al. 1968, Moran et al. 1968). The OH emission was found to have a source size of a few mas and $T_b \approx 10^{12}$ K (Moran et al. 1968).

Galactic maser sources are found in star formation regions near young stellar objects, such as proto-stars and compact HII regions, and in molecular envelopes of evolved stars, and they have been known since the 1960s at the beginning of molecular line radio astronomy (Reid & Moran 1981, Reid 2002). Both OH and H_2O maser sources in star formation regions tend to be more luminous than the evolved star variety, by a factor of about 100. The isotropic luminosity[3] for a H_2O maser source in the star formation region W49N can be as high as 1 $L_\odot$ integrated over the entire spectrum, and 0.1 $L_\odot$ in one spectral feature with a linewidth of 3.6 km^{-1} or 10 trillion trillion megawatt in a bandwidth of 270 kHz (Genzel & Downes 1977; Walker, Matsakis & Garcia-Barreto 1982).

With sufficient improvement in the detection sensitivity, OH and H_2O masers from star formation regions were also detected in nearby external galaxies

[2]Population inversion, maser and laser emission have also been found in the atmospheres of comets and planets (Mumma et al. 1981). In contrast to molecular masers, the Auroral Kilometric Radiation (AKR) observed from the Earth's upper ionosphere is a cyclotron maser arising from population inversion in the electron distribution driven by the loss-cone anisotropy (Wu & Lee 1979). Such cyclotron masers are believed to operate in other planetary magenetospheres, as well as in the solar corona and in other stars (Dulk 1985).

[3]The isotropic luminosity assumes that the maser emission is nondirectional. If a maser source is composed of a collection of individual maser "spots" that were directional, statistically such a collection may be expected to radiate in all directions. This argument is of course subject to experimental verification, and in some mega-masers, this assumption is clearly not correct.

(Whiteoak & Gardner 1973, Churchwell et al. 1977). Unexpectedly, very powerful H_2O and OH maser emission of the order of 10^6 times more luminous than typical Galactic masers were found in the nuclear regions of external galaxies (Dos Santos & Lepine 1979; Baan, Wood & Haschick 1982). They are termed "mega-masers" due to their very large inferred isotropic luminosity in the maser emission lines. The most distant OH mega-maser currently known is IRAS 14070+0525 at a redshift of $z = 0.265$ (Baan et al. 1992) and the most distant H_2O mega-maser known is at $z = 0.66$ (Barvainis & Antonucci 2005). Given the remarkable properties of these mega-masers, a number of questions arise, such as: How are the H_2O and OH mega-masers related to Galactic maser sources? What physical conditions can produce such luminous maser emission? How are they related to their host galaxies and what can they tell us about the host galaxies? Are they physically related to each other? How can their observations help us understand other astronomical problems? As will be seen in this review, the answers are rather rich.

Cosmic masers have been reviewed in the Annual Reviews roughly once every decade (Litvak 1974, Reid & Moran 1981, Elitzur 1992b). The present review will concentrate on the luminous H_2O and OH mega-masers that are found only in external galaxies, their properties, their origins and their applications as high-resolution probes of the most interesting regions in active galaxies and their potential use as tracers of and for studying galaxies at high redshift.

There were two conferences devoted exclusively to cosmic masers (Clegg & Nedoluha 1993, Migenes & Reid 2002) and an IAU Joint Discussion was devoted to mega-masers (Andersen 1998). Reviews of various aspects of mega-masers have been given by different authors (Baan 1985, 1996, 1998; Moran et al. 1995; Braatz, Wilson & Henkel 1996b; Greenhill 1997, 2002; Cohen 1998; Moran & Greenhill 1999; Moran 2000; Lonsdale 2002; Maloney 2002a; Watson 2002; Darling 2003; Henkel & Braatz 2003). There is also a textbook on Astronomical Masers (Elitzur 1992a).

1.1. Conditions for Maser Emission

Population inversion of the masering molecules and velocity coherence[4] along the line of sight through the inverted medium over a path length sufficiently long to achieve significant gain are the necessary conditions for detectable maser emission. Implicit in the population inversion condition is the presence of a nearby energy source. Achieving the population inversion of the maser levels is termed pumping of the maser, and energy from the energy source (stars in the case of Galactic masers) is converted to the maser emission by this pumping process. Pump mechanisms are classified as collisional or radiative, according to whether the energy transfer is from collisions or from absorption of radiation.

In collisional pumping, population inversion of the maser levels can be achieved by either of the following two cycles: (1) collisions bring the molecules to

[4]This means that the masering molecules must be at the same radial velocity to within the thermal width along the gain path in order to sustain stimulated emission.

high-lying states from which the spontaneous radiative decay into the upper maser level is faster than to the lower maser level, or (2) the spontaneous decay from the upper maser level to low-lying levels is slower than the spontaneous decay from the lower maser level, and collisions bring the molecules back to the upper maser level (Goldreich & Kwan 1974). If the H_2 gas density is much higher than the critical density (at which the inelastic collisional rate equals the radiative decay rate of the typically IR transitions in molecules; $n_{\rm crit} \sim 10^{11}$ cm^{-3} for the H_2O line), the population of the levels will be thermalized by collisions at $T_{\rm k}$, the kinetic temperature of the gas.

$$\frac{n_{\rm u}/g_{\rm u}}{n_{\rm l}/g_{\rm l}} = \frac{\gamma_{\rm lu}/g_{\rm u}}{\gamma_{\rm ul}/g_{\rm l}} \equiv \exp\left(-\frac{h\nu}{kT_{\rm k}}\right) < 1,$$

where $\gamma_{\rm lu}$ and $\gamma_{\rm ul}$ are the collisional coefficients of excitation and de-excitation, respectively. In this case, the population inversion will be destroyed and the maser emission is said to be quenched. In general, there may be trapping of the IR radiation (see below) in the maser source and there are more than a single transition, so that the critical density is somewhat model dependent (Kylafis & Norman 1991, Wallin & Watson 1997). So, maser sources have an upper limit to their high-gas density and increasing the density of the gas does not lead to unlimited increase of maser output. In radiative pumping, (*a*) there can be more transitions to high-lying states out of the upper maser level than from the lower maser level via absorption of (IR) photons, or (*b*) given equal absorptions from the maser levels to the high-lying levels, subsequent de-excitation can overpopulate the upper maser level. Radiative pumping by IR photons from sources external to the maser source tends to be less efficient than collisional pumping.

In both types of pumping mechanisms, there is always accompanying emission of IR photons to the maser emission. The maser source has to be optically thin to these IR photons, otherwise the trapping of these IR photons by the maser molecules effectively increases the radiative lifetime by the optical depth of the IR photons, thereby reducing the critical density and leading to thermalization of the population. Ultimately, the maser emission rate is limited by the loss or destruction rate of the accompanying IR radiation (Rank, Townes & Welch 1971). This condition constraints the geometry of the maser source because the surface area for cooling should be optimized, favoring an elongated or flat structure. Alternatively, there has to be some internal absorption mechanism, such as that due to cold dust within the maser source (Goldreich & Kwan 1974, Deguchi 1981, Collison & Watson 1995).

1.2. Pumping of H_2O Masers

The H_2O molecule is an asymmetric top, with the rotational levels specified by $J_{K_-K_+}$, where J is the total angular momentum, and K_- and K_+ are its projections on the largest and smallest principal axes, respectively (Townes & Schawlow 1955). The H_2O rotational energy levels are very rich, with most rotational transitions in the sub-millimeter and far-infrared wavelength range (Chandra, Varshalovich &

Kegel 1984; Neufeld & Melnick 1991). The 22.235 GHz ($\lambda = 1.35$ cm) transition is between the 6_{16} and 5_{23} levels that happen to lie very close to each other in energy.

Population inversion between the 6_{16} and 5_{23} levels of H_2O can result from collisional pumping (de Jong 1973). The 6_{16} level, the lowest of the J = 6 ladder, is strongly coupled to the corresponding lowest J states. These backbone states are overpopulated relative to other states, leading to population inversion with another neighboring state if the selection rules of the transition are satisfied. Given that the 6_{16} level lies at $E/k = 643$ K above ground, collisions with high-density gas [$n(H_2) \sim 10^8$ cm^{-3}] at a temperature of >300 K are required (Kylafis & Norman 1991). The critical density for the 22 GHz H_2O line is $\sim 10^{11}$ cm^{-3}. Subsequent calculations for different physical settings and improved collisional cross sections (Deguchi 1981; Elitzur, Hollenbach & McKee 1989; Neufeld & Melnick 1991) all show that collisional pumping can invert the populations of the 6_{16} and 5_{23} levels for the 22.235 GHz maser emission, and that maser emission between other levels is also indicated.[5]

1.3. Pumping of OH Masers

OH has an unclosed shell of electrons and the ground electronic state is a Π-state, with electronic angular momentum $L_z = 1$. Because of the unpaired electron, $S = 1/2$ so that the total angular momentum $J_z = 1 \pm 1/2$, leading to the two rotational ladders, $^2\Pi_{3/2}$ and $^2\Pi_{1/2}$ (Figure 1). The coupling of the electronic angular momentum and the rotation of the molecule introduces a splitting of all the rotational states, called Λ-doubling. Finally, coupling of the spin of the unpaired electron with the nuclear spin of the H atom introduces hyperfine splitting in all the levels. Each hyperfine level is characterized by the quantum number F, the sum of the nuclear and electronic spins.

The λ18 cm lines correspond to the four possible transitions between the hyperfine levels in the Λ-doublet of the ground rotational state $^2\Pi_{3/2}(J = 3/2)$, with frequencies at 1612, 1665, 1667, and 1720 MHz and the corresponding line strengths in the ratio of 1:5:9:1. The various rotational levels are connected by far-IR lines. The allowed transitions follow the dipole selection rules, which require a parity change and $\Delta F = 0, \pm 1$ (but $F = 0 \rightarrow 0$ is forbidden). The population of the magnetic sub-states in the ground rotational level is different by less than 1 part in 10^4 at a typical temperature of 100 K, given the Λ-doublet splitting $\Delta E/kT \approx 0.00013$. If the upper Λ-doublets are inverted relative to the lower doublets, then all four transitions could be masering, which is essentially never observed. This indicates the inversion mechanism is not simple (Elitzur 1992).

Theoretical models have shown that radiative excitation accompanied by collisional de-excitation tends to invert the hyperfine levels within the $^2\Pi_{3/2}$ ladder. The

[5]Sub-millimeter water maser emission between other levels has been observed: $10_{29} \rightarrow 9_{36}$ at ~321 GHz (Menten, Melnick & Phillips 1990), $5_{15} \rightarrow 4_{22}$ at ~325 GHz (Menten et al. 1990), $3_{13} \rightarrow 2_{20}$ at ~183 GHz (Cernicharo et al. 1990), $1_{10} \rightarrow 1_{01}$ of $\nu_2 = 1$ vibrational state at ~658 GHz (Menten & Young 1995).

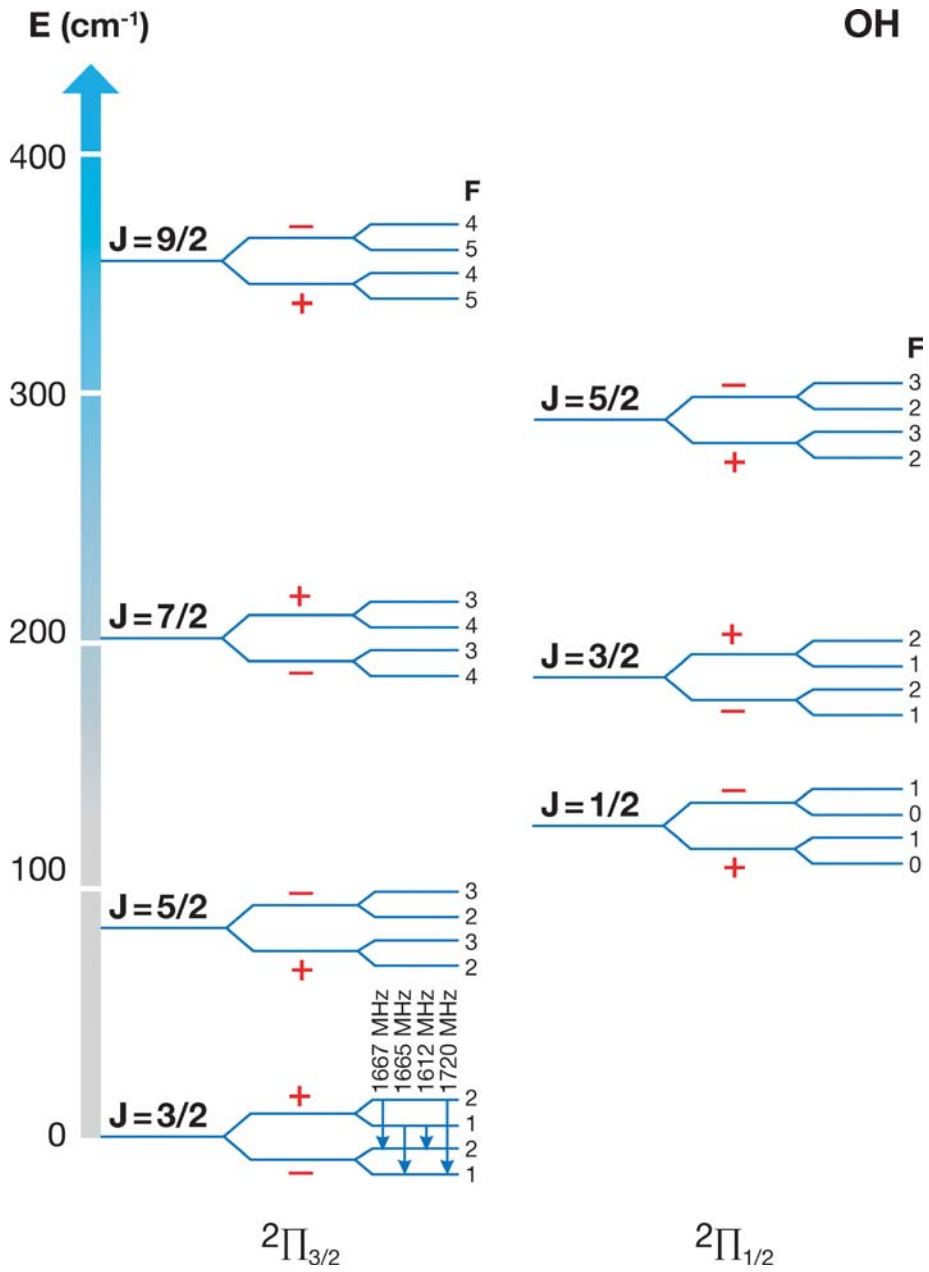

Figure 1 OH energy diagram showing the λ18 cm transitions between the hyperfine levels in the ground state ($^2\Pi_{3/2}$ $J = 3/2$). Similar transitions in the $^2\Pi_{3/2}$ $J = 5/2$ and $^2\Pi_{1/2}$ $J = 1/2$ states ($F = 0 \rightarrow 0$ transition not allowed) have wavelengths near 6 cm and 5 cm, respectively.

appropriate conditions can be obtained with gas temperature of ∼160 K, a column density of $N_{OH} \approx 10^{17}$ cm^{-2}, gas density $n_{H_2} \leq 10^7$ cm^{-3}, and a dust temperature slightly higher than the gas temperature (Cesaroni & Walmsley 1991, Kylafis & Norman 1990). However, such high-temperature dust is typically not seen in the general interstellar medium. The IR spectral energy distribution of dust emission from star forming regions typically peaks at 60 μm to 100 μm, corresponding to much lower dust temperature, at 30–50 K. This suggests that the source of OH maser emission has to be quite close to the energy and heating source, and therefore spatially relatively confined.

The pumping mechanism for OH maser emission appears to depend more directly on far-IR radiation than that for H_2O masers, which are collisionally pumped. As we shall see, the environments in which the OH and H_2O mega-masers are found may reflect the different pumping mechanisms for the two kinds of masers.

1.4. Abundance of Interstellar H_2O and OH

The existence of interstellar H_2O and OH maser emissions is predicated on the gas phase abundance of H_2O and OH in the masering medium, presumably in molecular clouds. The steady state ion-molecular chemistry predicts that H_2O, along with O_2, CO and O, are the gas-phase reservoir of elemental oxygen in molecular gas that is well shielded from ultra-violet radiation, e.g., (Millar 1996). OH is formed from the dissociation of H_2O, such as in photon dominated regions (PDRs) (Hartquist et al. 1995, Hollenbach & Tielens 1997), or in the shocked gas as a magneto-hydrodynamic shock wave propagating in a molecular cloud (Draine, Roberge & Dalgarno 1983).

However, recent *Submillimeter Wave Astronomy Satellite* (SWAS) results indicate that gas-phase H_2O (and O_2) is deficient in most regions in the Galaxy: $10^{-9} < x(H_2O) \equiv [n(H_2O)/n(H_2)] <$ a few $\times\, 10^{-8}$ in extended regions of molecular clouds and $x(H_2O) < 7 \times 10^{-8}$ in starless cores in molecular clouds, while the abundance is high in diffuse gas (Snell et al. 2000a,b,c). In regions with active star formation, ISO observations have revealed abundant gas phase water ro-vibrational and rotational lines, implying the water abundance ranges from 10^{-5} to a few $\times 10^{-4}$ (van Dishoeck 2001). The most promising model to account for these results is that in dark clouds, gas grain chemistry and freeze-out onto grains convert O and C into solid H_2O and CH_4. H_2O remains strongly bound to the surface of grains and evaporates when $T_{dust} > 100$ K (Bergin et al. 2000), in the presence of heating by newly formed stars.

Thus, the existence of OH and H_2O maser emissions would require the appropriate physical conditions to release the H_2O molecules from the grains into the gas phase, as well as the photodissociation of H_2O in the case of OH masers. The association of OH maser sources with ultra-compact HII regions and of H_2O masers with proto-stellar objects are consistent with the current understanding of the chemistry of OH and H_2O in the interstellar medium. In the case of OH mega-masers, if the OH amplifying medium is extended, the conditions for photodissociation of H_2O over a large region would also be required.

2. OH AND H_2O MASER SOURCES IN THE GALAXY

In the Galaxy, OH, H_2O, SiO and CH_3OH masers are widespread, but they can be classified as either interstellar or circumstellar (Reid 2002). The interstellar masers originate in dense molecular gas in star formation regions (Lo 1974, Genzel et al. 1978), closely associated with ultra-compact HII regions, embedded IR sources, hot molecular cores, Herbig-Haro objects, and outflows. Figure 2 shows

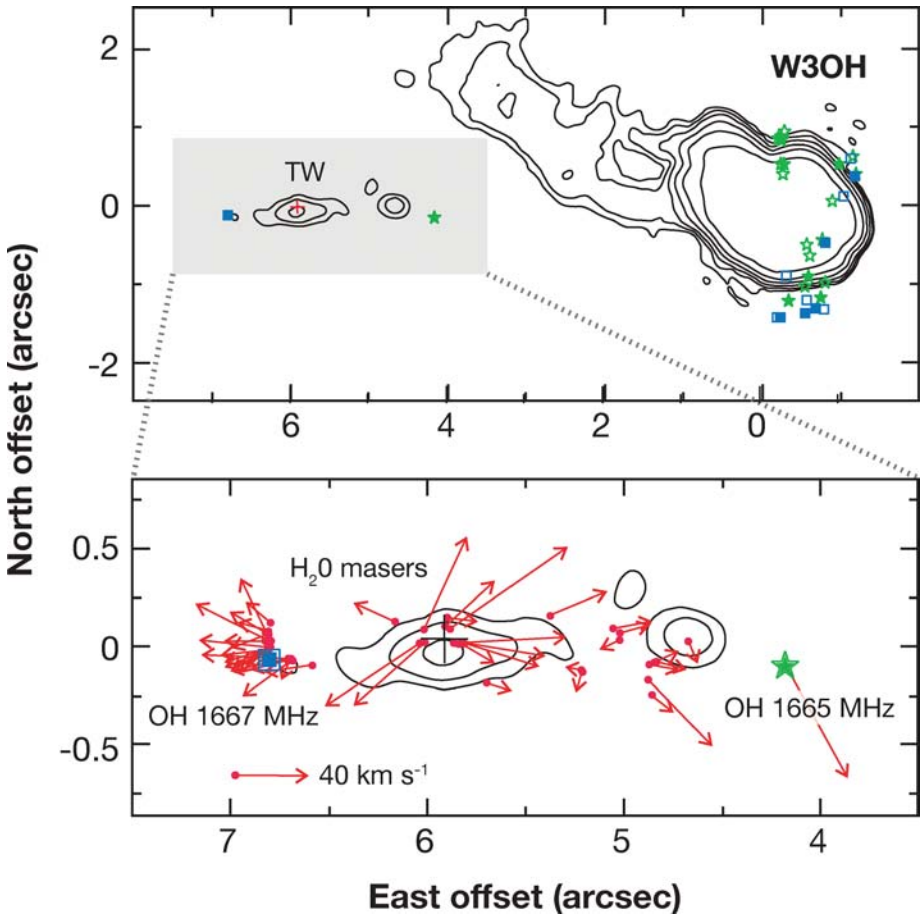

Figure 2 The two panels display VLA maps of the radio continuum emission (in *contours*) from the galactic compact HII region: W 3(OH), showing the relationship of interstellar OH and H_2O maser sources. The *stars* represent 1665 MHz OH maser emission and the *squares* 1667 MHz OH maser emission. *Open symbols* are RCP and *closed symbols* LCP. Positions and proper motions of the H_2O masers are indicated by *filled circles* and *arrows*, respectively. $1''$ corresponds to 3000 AU, or 1.5×10^{16} cm (Argon, Reid & Menten 2003).

the physical relationship and the size scale of OH and H_2O masers and ultra-compact HII regions. Both the OH and H_2O maser emissions originate from very compact spots of dimension $\sim 10^{13}$ cm spread over an extent $\sim 10^{17}$ cm in the immediate vicinity of IR sources or compact HII regions, both excited by very young stellar objects. The velocity spread of the emission from each spot is narrow, ~ 1 km s^{-1}. OH masers with only 1720 MHz emission appear to be associated with supernova remnants (Greenhill et al. 2002). Circumstellar masers of SiO, H_2O, and OH originate in the molecular circumstellar envelopes of evolved giant and super-giant stars.

All maser sources are found in high-density molecular gas, in the vicinity of an energy source that provides the energy for pumping the population inversion, either by radiation or collisions, often mediated by shocks in the medium. In terms of energetics, the isotropic luminosity of circumstellar H_2O masers has a mean of $10^{-6}\ L_\odot$, but can reach $10^{-4}\ L_\odot$. Interstellar H_2O masers are more energetic, with a mean luminosity of $10^{-4}\ L_\odot$, reaching as high as $\sim 1\ L_\odot$ (Palagi et al. 1993).

3. EXTRAGALACTIC H_2O MASER EMISSION

Detecting H_2O masers from external galaxies was originally mainly limited by sensitivity. Placing the strongest known galactic interstellar maser, with a luminosity of $1\ L_\odot$, at the distance of the nearest galaxies yields an estimated flux density of the order of 1 Jy, a signal that is detectable with the combination of sensitive amplifiers, 40-m to 100-m diameter telescopes, and spectrometers available beginning in the late 1970s. As Galactic interstellar masers were largely found toward HII regions, the typical strategy was to search for H_2O masers from known HII regions in the nearest galaxies (Dickinson & Chaisson 1971, Andrew et al. 1975), and later from irregular and blue compact dwarf galaxies (Huchtmeier, Eckart & Zensus 1988; Becker et al. 1993).

The first extragalactic H_2O maser emission detected was toward the giant HII region IC 133 in the disk of M 33 with the Effelsberg 100-m radio telescope in Bonn (Churchwell et al. 1977). The maser emission properties were similar to the interstellar masers found in the Galaxy. Subsequently, maser emission with luminosity comparable to the Galactic masers was found in other regions of M 33 and IC 342 (Huchtmeier et al. 1978).[6]

In 1979, unexpectedly strong emission (10 Jy) from an edge-on galaxy, NGC 4945, was detected using the 13.7-m telescope at Itapetinga Brazil (Dos Santos & Lepine 1979). The source was the most powerful H_2O maser known at that time, 10 times more luminous than the brightest maser in the Galaxy. Subsequently, in a survey of Southern galaxies with the Parkes 64-m telescope,

[6]By now, such masers are found in several nearby galaxies, including SMC (Scalise & Braz 1982), LMC (Scalise & Braz 1981, 1982; Whiteoak et al. 1983; Whiteoak & Gardner 1986; van Loon & Zijlstra 2001), IC 10 (Henkel, Guesten & Batrla 1986) and IC 342 (Tarchi et al. 2002b).

a second intense nuclear H_2O emission source was detected from the Circinus galaxy. It was suggested that the powerful maser arose from extended regions of high-density and high-radiation fields, powered by hot young stars, in a large molecular cloud at the galactic nucleus (Gardner & Whiteoak 1982).

With a new sensitive maser receiver and a new wide-band acoustic-optic spectrometer, a survey of nearby galactic nuclei was started in late 1982 with the Owens Valley Radio Observatory 40-m telescope to look specifically for luminous extragalactic masers such as those in the nuclei of NGC 4945 and the Circinus galaxies. Four new extragalactic water maser sources—NGC 4258, NGC 1068, M 82 and NGC 6946—were detected out of an initial survey of 29 nearby late-type galaxies reaching a 3-σ detection limit, δS_ν, of $\sim$0.2 Jy (Claussen, Heiligman & Lo 1984; Claussen & Lo 1986). Two of them had luminosities $\gg 1\ L_\odot$: NGC 1068 (450 $L_\odot$) and NGC 4258 (120 $L_\odot$).

3.1. Luminous Nuclear H_2O Masers: Circumnuclear Versus Interstellar

The unexpectedly large luminosity, ranging up to 450 $L_\odot$, of the extragalactic nuclear water masers indicates that these masers have unusual properties. Empirically, the luminosity function of Galactic interstellar masers shows that the mean luminosity is $10^{-4}\ L_\odot$ with only a couple known to have luminosity larger than 0.1 $L_\odot$ (Palagi et al. 1993). The brightest Galactic water maser source, W 49N, is highly variable, and one of the peaks or "features" of its spectrum at a given velocity with a width of 1 km s^{-1} can reach a maximum luminosity of $\sim 1\ L_\odot$. As it is not easy to account for maser emission of up to 1 $L_\odot$ (Strelnitskii 1984), the problem is even more exacerbated in the case of the extragalactic luminous water masers (Moran 1984).

Initially, the high luminosity of the nuclear maser emission was attributed to the large number ($N \geq 10^3$) of W 49N-like interstellar masers in the nuclear star-burst regions (Gardner & Whiteoak 1982; Claussen, Heiligman & Lo 1984). However, high-angular resolution observations of two of the sources with the Very Large Array (VLA) showed that the luminous masers were unresolved by the 70 mas beam, corresponding to 1–3 pc in size, suggesting a very high concentration of young massive stars. Furthermore, the water maser emission from NGC 4258 and NGC 1068 was observed to vary significantly on the time scale of months. The observed variability therefore ruled out the model that the luminous water maser emission is due to the sum of a large number of independent masers, each powered by one of the large number of young stars in a starburst region. Under this model, the expected fractional variability would go as $N^{-1/2} < 10^{-1}$, much smaller than what is observed (Claussen & Lo 1986).

The specific intensity of the emission emerging from a maser source with gain length L and surface area $\sigma (= \mathrm{d}^2)$ is given by

$$I_\nu = \frac{n_\mathrm{u} \sigma L h\nu \Delta P}{\sigma \Delta\nu \Delta\Omega} = \frac{n_\mathrm{u} \Delta P h\nu L^3}{\sigma \Delta\nu}\ \mathrm{erg\,s^{-1}\,cm^{-2}\,Hz^{-1}\,str^{-1}},$$

where n_u is the density of water molecules in the upper state, $\sigma\ L$ is the volume of the maser source, ΔP is the pump rate of population inversion, and $\Delta\nu$ and $\Delta\Omega\ (=\sigma/L^2)$ are the bandwidth and the emerging solid angle of the emission, respectively (Strelnitskii 1984). This is in the limiting case of a saturated maser, in which the maser photon emission rate is equal to the pump rate, at the maximum efficiency of converting the input power to maser emission. The observed flux density is then

$$S_\nu = I_\nu \left(\frac{\sigma}{D^2}\right) = \frac{n_u \Delta P h \nu L^3}{D^2 \Delta \nu}\ \mathrm{erg\,s^{-1}\,cm^{-2}\,Hz^{-1}}.$$

Aside from the obvious inverse square dependence of distance D, if the luminous masers are in physical environments with comparable n_u and ΔP to Galactic masers, the key variable determining the flux density is the cubic dependence of the gain length, L^3. The flux density of a maser is very sensitively dependent on the gain length, and therefore the dimension, of the maser.

Given this sensitive dependence on dimension, a model of the luminous extragalactic water masers is needed in which high-density gas is found in a setting with larger scale-size than masers near stars. Inspired by the parsec scale of a circumnuclear disk proposed to explain the polarized optical continuum and broad emission lines from active galactic nuclei (Antonucci & Miller 1985), and in analogy with the circumstellar disk proposed to explain masers around proto-stars (Elmegreen & Morris 1979), it was proposed that the luminous water masers could originate in dense gas clouds in a circumnuclear disk excited by mass outflow from an active nucleus (Claussen & Lo 1986). The key point of this model is that nuclear H_2O masers are qualitatively different from Galactic masers, because they originate in circumnuclear dense clouds and the ultimate energy source is the active galactic nucleus (AGN), instead of stars in the case of the Galactic masers.

This suggestion was difficult to prove and was not widely accepted at the outset. For example, it was argued that luminous masers are just the extreme luminous end of a distribution of Galactic type interstellar masers (Ho et al. 1987). To explain OH mega-masers, background radio continuum emission being amplified by a foreground medium with population inversion had been proposed and the same model was extended to luminous H_2O masers (Baan, Schmelz & Haschick 1985). As an example, the "periodic" intensity variability of NGC 4258 was attributed to the amplification by the molecular envelope of a variable star that happens to sit in front of the radio continuum of NGC 4258 (Baan & Haschick 1990).

4. NGC 4258: ARCHETYPAL CIRCUMNUCLEAR H_2O MASER

The suggestion that luminous masers are associated with circumnuclear dense molecular clouds had no definitive observational support until three independent pieces of evidence on the maser emission from NGC 4258, gathered over a period from 1984 to 1992, were combined. They consist of (*a*) results from a 1984 VLBI

observation showing the linear distribution of the main emission features with a constant velocity gradient (Greenhill et al. 1995b), (*b*) the observation of increasing velocity linearly with time of the maser spectral features near the systemic velocity between 1984 and 1986 (Figure 3) (Greenhill et al. 1995a), and (*c*) the detection of high-velocity emission at ± 900 km s^{-1} from the systemic velocity (Figure 4*a*) (Nakai, Inoue & Miyoshi 1993).

VLBI observations of the maser emission from NGC 4258 were first made in 1984 and preliminary results were reported in 1986 (Claussen et al. 1988). Since the high-velocity emission was not known in 1984, only the main features were observed. The main features were found to originate from a linear spatial distribution with a constant velocity gradient along it, suggesting a rotating source

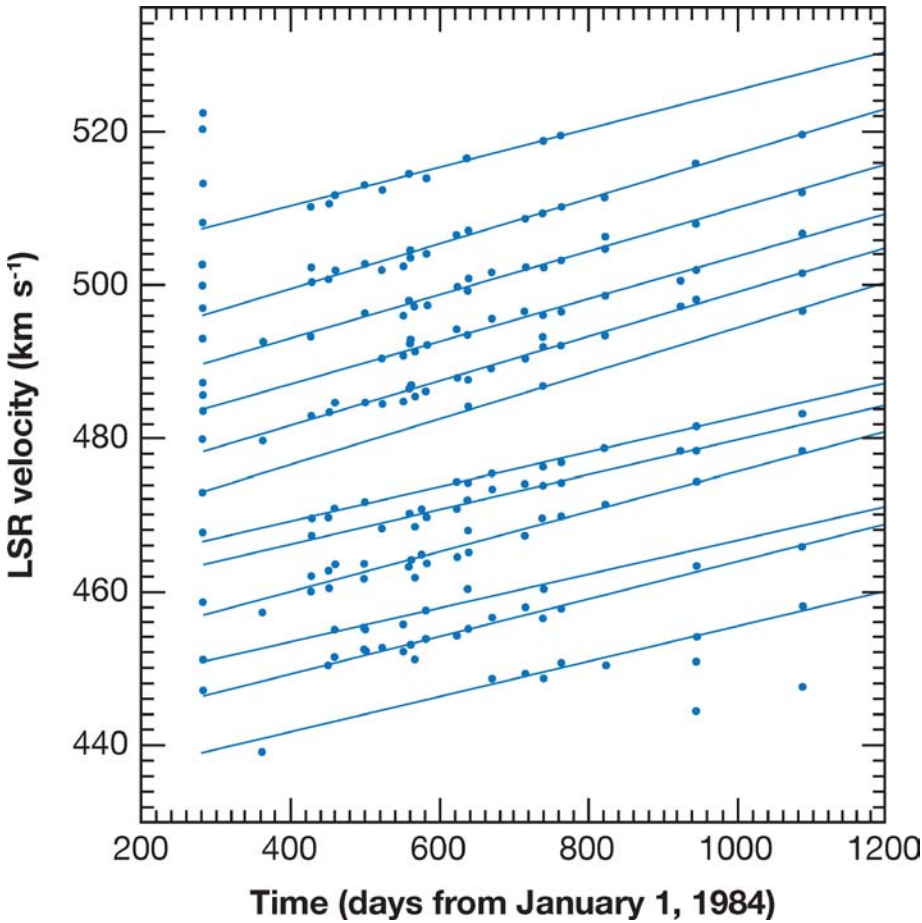

Figure 3 A plot versus time of the velocities of the spectral features near the systemic velocity of the luminous H_2O maser in NGC 4258 (Greenhill et al. 1995a). The mean rate of increase is 9.5 ± 1.1 km s^{-1}/year.

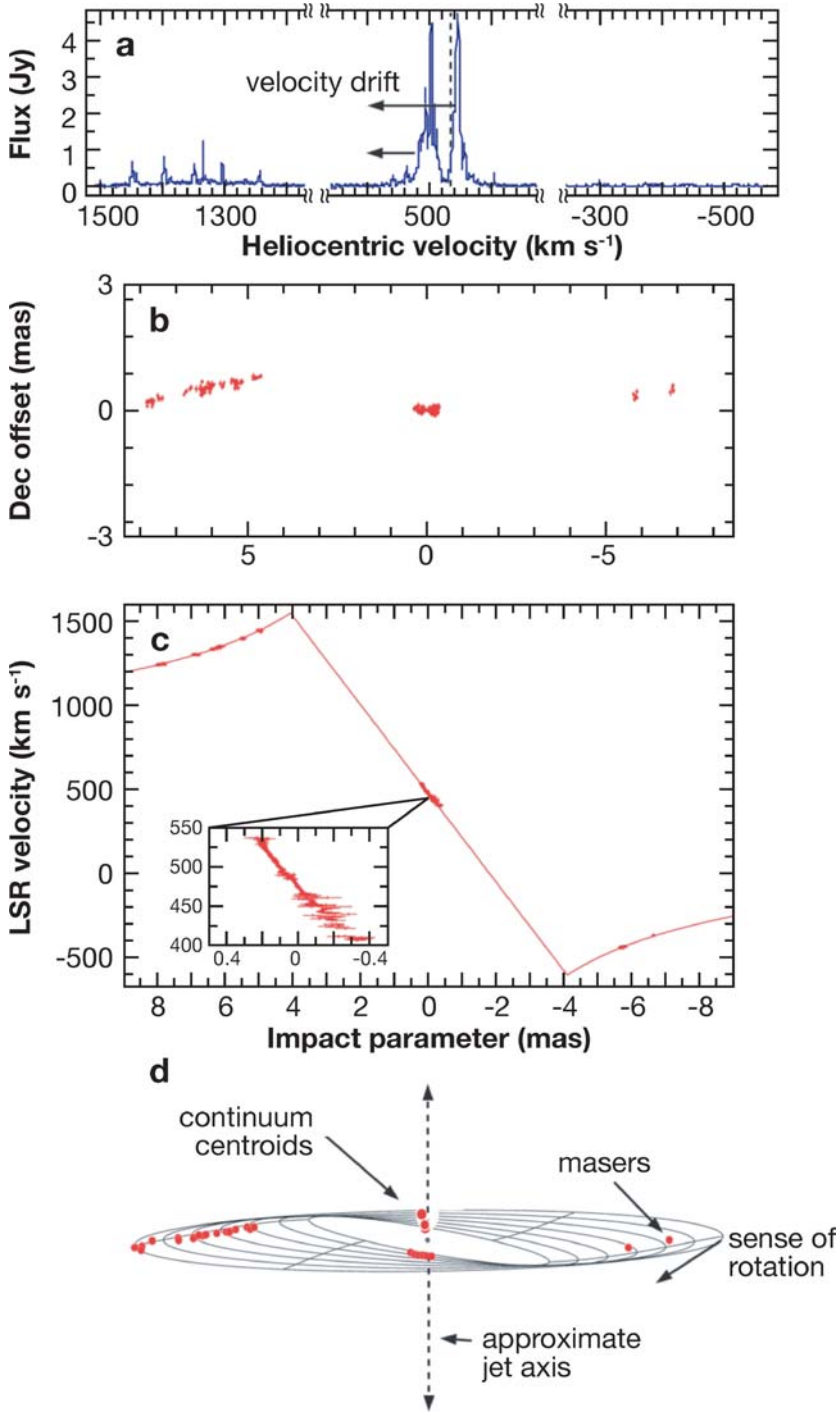

(Greenhill et al. 1995b). However, if one fits the standard rotating "ring" to the observed spatial distribution of the main features, one would obtain a small ring, with low-rotational velocity and small enclosed mass.

The maser emission in NGC 4258 was monitored at high-spectral resolution between October 1984 and December 1986 by R. Becker and C. Henkel at the Effelsberg 100-m telescope for variability. While intensity variability had been observed ever since the discovery of the source, an interesting pattern became apparent when the peaks of the spectra were plotted in a diagram that shows the velocity of the spectral peaks on the vertical axis and the epoch of observation on the horizontal axis by R. Becker (C. Henkel, private communication) (Greenhill et al. 1995a). The pattern showed the velocity of the peaks in the spectra increasing linearly with time. A similar pattern was also present in a more extensive set of monitoring observations from 1983 through 1993 with the Haystack 37-m telescope (Haschick, Baan & Peng 1994).

With a very wide band acousti-optic spectrometer covering 3850 km s^{-1} (or 285 MHz) instantaneously, maser emission was detected from NGC 4258 at velocities ranging up to ± 900 km s^{-1} from the systemic velocity. The high-velocity emission was not discovered previously because spectrometers used before covered too narrow a velocity range. Three possible explanations were offered for the high-velocity emission: (*a*) masers orbiting a massive central black hole, (*b*) ejecta in a bipolar outflow, and (*c*) frequency up- and down-shifted Raman scattering in a dense plasma (Deguchi 1994). The high-velocity emission, with the luminosity ranging between 0.1 to 6 $L_\odot$ integrated over the linewidth, was determined to come within $0.05''$ of the main features (Nakai, Inoue & Miyoshi 1993).

4.1. A Rotating Disk Model

Independently, each of the three pieces of evidence was puzzling and inconclusive. Together, they are very naturally explained by a rotating disk model (Watson & Wallin 1994). In such a model, the maser emission features at the systemic velocity arise just in front of the central continuum source and the high-velocity emission, at $\pm V_{\rm HV}$ relative to the systemic velocity, arises from points of the disk tangent to the line of sight on either side of the center, all at roughly the same radius from the center. It is easy to see that the rotational velocity at radius r is $V_{\rm r} = V_{\rm HV}$. The constant rate of the velocity increase of the systemic velocity features is due to their centripetal acceleration: $\frac{{\rm d}V}{{\rm d}t} = \frac{V_{\rm r}^2}{R}$. The constant velocity gradient

←

Figure 4 NGC 4258: The *top panel* (*a*) shows the spectrum of the luminous H_2O maser; *panel* (*b*) shows the spatial distribution of the maser emission; *panel* (*c*) shows the rotation curve of the maser emission; *panel* (*d*) shows a 3D model of a warped thin disk fitted to the spatial distribution of the maser emission shown in (*b*) (Bragg et al. 2000).

$\frac{dV}{d\theta} = D \times \frac{dV}{db} = D \times \frac{V_r}{R}$, where the impact parameter from the central source, b, equals the angular offset from the center θ times the distance D. Furthermore, with three unknowns to the model—R, V_r, D, and three observables—V_{HV}, dV/dt, and $dV/d\theta$, the distance to the source can also be determined. A similar model was presented subsequently (Haschick, Baan & Peng 1994).

Despite this most appealing explanation, the circumnuclear nature of the luminous H_2O maser in NGC 4258 still needed verification by observations, since the position of the high-velocity emission was not known. The ultimate proof of a circumnuclear maser disk in NGC 4258 came from the remarkable results of the VLBA (Very Long Baseline Array, operated by the National Radio Astronomy Observatory) observations of the high-velocity emission along with the main maser features (Miyoshi et al. 1995), which is described in detail below.

4.2. Observation of a Circumnuclear Maser

The VLBA observations (Miyoshi et al. 1995, Moran et al. 1995) showed that the high-velocity features are spatially offset from the features at the systemic velocity which are distributed in a nearly planar structure (Figure 4*b*), and the velocity of the high-velocity features decreases with distance (r) from the center of rotation as $r^{-1/2}$ (Figure 4*c*). The results can be interpreted as the high-velocity emission arising from points tangent to the line of sight on opposite sides of a nearly edge-on thin Keplerian disk, between the inner and outer radii of 0.13 pc and 0.26 pc, respectively (Figure 4*d*). The inclination angle of the disk is $\sim 83^\circ$, deduced from the displacement of the systemic features from the line between the high-velocity features. The rotational axis of the disk is offset from the rotational axis of the galaxy by 119° (counter-rotating). The deviation of the high-velocity features from a straight line passing through the systemic features suggests that the rotating disk is warped.

The restricted distribution of the maser emission can be understood as due to the lines of sight offering the longest path with zero velocity gradient which is required for stimulated emission: the line of sight to the center through the disk at the systemic velocity, and the tangent lines perpendicular to the radial lines on the sides of the disk at high velocities. In the Keplerian disk of NGC 4258, the velocity coherent path length at the tangent points at radius R is $2(\delta V/V)^{1/2}R \sim 10^{16}$ cm for a velocity change of a typical maser linewidth of 1 km s^{-1}.

In short, the VLBA observations of the H_2O mega-maser in NGC 4258 constitute to date the most compelling direct observational evidence for the existence of a thin Keplerian molecular accretion disk in a galactic nucleus, in strong support of the long standing paradigm of accretion of matter by a super-massive black hole (see below) to power quasars and AGNs (Salpeter 1964, Lynden-Bell 1969).

4.3. Evidence for a Massive Black Hole

Despite the attractiveness and common acceptance of the picture that quasars and AGNs are powered by gravitational energy extracted from the accretion of

matter by a super-massive black hole, the proof of the existence of a super-massive black-hole has been difficult to establish (Kormendy & Richstone 1995). Strictly speaking, one has to establish the mass to radius ratio, M/R, of the black-hole candidate to be equal to $M/R_{sc} \equiv c^2/2G = 6.7 \times 10^{27}$ g/cm, where R_{sc} is the Schwarzschild radius and G is the gravitational constant. One practical limitation is the very high angular resolution required to probe close to R_{sc}. For example, $R_{sc} \approx 2$ AU for a 10^8 $M_\odot$ black hole subtends 0.2 μas at 10 Mpc.

The combination of the high-brightness temperature of circumnuclear water maser emission in NGC 4258 and the high-angular resolution of VLBI has enabled the probing of an AGN at 7 Mpc with $\sim$300 μas resolution, which is difficult to achieve by other means. The Keplerian rotation curve of the circumnuclear maser disk defines a spherical distribution of mass of 3.7×10^7 $M_\odot$ within 0.13 pc of the center, implying an average mass density of 4×10^9 $M_\odot$ pc^{-3}. This also corresponds to a M/R of 2×10^{25} g/cm.[7] Since it is very difficult to account for the deduced average mass density in the central 0.1 pc of NG4258 by a compact cluster of stars because of dynamical instability (Maoz 1995), the astronomical case for a super-massive black hole is very compelling, even if the physics case is not proven yet. The circumnuclear H_2O masers are excellent systems in which similar determination of the central mass can be determined and the identification of more systems similar to the one in NGC 4258 is clearly important.

4.4. Properties of a Thin Accretion Disk

The accretion disk involved in the massive black hole paradigm has dimensions of the order of 1 pc which subtends a very small angle, such as $\sim$10 mas at a distance of 15 Mpc, requiring very high-resolution observations to detect directly. The existence of a circumnuclear torus has been inferred from spectro-polarimetric observations, and together with the unification scheme for Seyfert galaxies both point to the presence of a circumnuclear dusty and molecular disk or torus (Antonucci 1993). The *Hubble Space Telescope* has shown the presence of dust disks in a number of galaxies, but at the 100 pc to kpc scale. The H_2O mega-maser from NGC 4258 provides the first direct observational verification of a thin molecular accretion disk in Keplerian rotation about an AGN.

Observations of the mega-maser emission provide the following parameters of the accretion disk in NGC 4258 directly (Moran et al. 1995). Besides the inner radius, $R_i \sim 0.13$ pc, and the outer radius, $R_o \sim 0.26$ pc, and the Keplerian rotation curve, the spatial map of the maser emission directly provides deviations perpendicular to the major axis and is consistent with all the maser features being in the plane of the disk, indicating the vertical thickness H of the masering medium in

[7]For the Galactic center, where the stellar kinematics around Sgr A* also provides very compelling evidence for a super-massive black hole (Eckart, Ott & Genzel 1999; Ghez et al. 1998; Schödel et al. 2003), the average space density is 9.3×10^9 $M_\odot$ pc^{-3}, but M/R is only 4.2×10^{23} g/cm.

the disk is <0.01 mas or <0.0003 pc. If the thickness of the disk is the same as the thickness of the maser source (see also Neufeld & Maloney 1995) and the disk is supported under hydrostatic equilibrium vertically, then

$$\frac{H}{R} = \frac{c_s}{v_\phi} < 0.0025,$$

where c_s and v_ϕ are the sound speed and the Keplerian rotational speed, respectively. Thus, the value of H implies that $c_s < 2.5\,\mathrm{km\,s^{-1}}$. This suggests the gas temperature $T < 1000$ K if c_s is the thermal sound speed. The excitation of the H_2O maser levels requires the temperature of the gas to be $\geq$300 K ($c_s \geq 1.5$ km s^{-1}) and the density to be $\sim 10^9$ cm^{-3}. However, if the vertical support is provided by magnetic pressure, then c_s equals the Alfven speed $V_A = B/(4\pi\rho)^{1/2}$, implying a magnetic field of <55 mG.

The Zeeman-splitting induced circular polarization of the maser emission can be used to infer the magnetic field strength of the maser medium, which is taken to be the molecular accretion disk. A 1-σ upper limit of 300 mG has been derived for the parallel, or toroidal, component of the B field (Herrnstein et al. 1998b). A more recent result has reduced the upper limit to the toroidal component of the magnetic field in the accretion disk in NGC 4258 at a radius of 0.2 pc to 50 mG (Modjaz et al. 2003).

If self-gravity of the disk is negligible, as in this case of a thin Keplerian disk, the ratio of the disk mass to the central mass is small: $\frac{M_d}{M} \ll \frac{H}{R}$. This provides an upper limit to the disk mass: $M_d \leq 10^5 M_\odot$. To fit the spatial distribution of the maser emission precisely, a warp in the rotating disk has to be introduced (Neufeld & Maloney 1995). In a thin but optically thick accretion disk, radiation pressure from the central source can drive a warping instability even from an initially flat disk, because the back reaction of the radiation from the centrally illuminated warped disk surface provides the requisite torque (Pringle 1996; Maloney, Begelman & Nowak 1998). An alternate mechanism for the warp was proposed to be provided by a binary companion with a mass comparable to the disk (Papaloizou et al. 1998). The large-scale radio structure in NGC 4258 is suggestive of a precessing source of outflow (Wilson, Yang & Cecil 2001), and it would be interesting to investigate the connection of the large-scale radio structure to the precession of the warped disk.

The accretion disk in NGC 4258 where the maser emission arises is clearly molecular, but it is well known that molecular viscosity does not explain the viscosity needed in an accretion disk. Whether the accretion disk possesses turbulent motion is of interest to understanding the source of the viscosity. By comparing the observed H_2O maser spectra to simulated spectra of maser radiation in a thin Keplerian disk viewed edge-on with turbulent velocities present, it is possible to infer the magnitude of the turbulent velocities. It was found that with rms turbulent velocities comparable to the sound speed ($c_{turb} \sim c_s$) spectra similar to those actually observed can be constructed (Wallin, Watson & Wyld 1999).

As H_2O maser emission is not representative of the cooling rate from the disk and thermal radiation from the disk has not been observed directly, it is hard to draw firm conclusions on the viscosity and accretion rate of the disk. Furthermore, while the circumnuclear Keplerian thin disk between 0.13 pc and 0.26 pc of the nucleus of NGC 4258 is observationally constrained, how the accretion disk actually continues inwards is ambiguous. For example, the disk traced by the maser emission can extend to the central object so that the central engine is fueled by an optically thick, geometrically thin accretion disk (Neufeld & Maloney 1995), or there could be an optically thin advection-dominated flow (ADAF) at radii within 0.13 pc (Lasota et al. 1996). The inferred accretion rate is highly model dependent, and observations to further constrain the inner accretion flow are needed for a better estimate of the accretion rate (Maoz & McKee 1998; Gammie, Narayan & Blandford 1999). A 3σ upper limit of 200 μJy on any compact 22 GHz continuum emission coincident with the central engine in NGC 4258 implies that the inner ADAF flow cannot extend significantly beyond $\sim 10^2\ R_{sc}$ or 0.0004 pc (Herrnstein et al. 1998a).

4.5. Geometric Distance Determination

The extragalactic distance scale is fundamental to our understanding of the age, geometry and fate of the Universe, but it is very difficult to determine accurately, because of, for example, the assumption of standard candle based on the period-luminosity relationship of Cepheid variables (Hodge 1981, Teerikorpi 1997, Madore et al. 1999). Valiant efforts have been devoted to measure the proper motion of extragalactic H_2O masers due to the rotation of the parent galaxy, such as M33, in order to measure the distance to the galaxy (Brunthaler et al. 2002, Argon et al. 2004). The luminous H_2O maser from the circumnuclear Keplerian rotating disk in NGC 4258 provides an excellent system for the geometrical distance determination to an external galaxy, especially given the strong lines since the accuracy of proper motion measurements increases with their signal-to-noise ratio, S/N: $\delta\theta = \theta_b/(S/N)$, where $\delta\theta$ and θ_b are the error of proper motion measurements and the resolution of the observations, respectively.

Under the model in which the H_2O maser emission at the systemic velocity of NGC 4258 traces the circular orbital motions of discrete clumps of gas, the proper motion (31.5 μas year^{-1}) and the acceleration (9.3 km s^{-1} year^{-1}) of these clumps measured over time provide a determination of the distance to the nucleus of NGC 4258 of 7.2 ± 0.5 Mpc, where the uncertainty includes statistical errors of tracking the orbital motions of the masers, systematic errors from the uncertainties of the disk parameters, and the uncertainty in the eccentricity of the orbit (Herrnstein et al. 1999). This is the most precise determination of an extragalactic distance so far. Clearly, extending such measurements to more galaxies and to larger distances is very important, providing another strong motivation for searching for additional luminous circumnuclear H_2O masers similar to NGC 4258.

5. SEARCHES FOR H_2O MEGA-MASERS

In the last two decades, sustained and extensive efforts have been devoted to searches for luminous water masers from various samples of galaxies. Given the association of interstellar masers with star forming regions in the Galaxy, searches were initially directed toward galaxies with indicators of enhanced star formation. A survey of "star-burst" galaxies and galaxies with radio emission was carried out with the Haystack 37-m telescope ($\delta S_\nu = 0.5$–1.5 Jy), resulting in the detection of NGC 3079 with a luminosity of $\sim$500 $L_\odot$ (Haschick & Baan 1985). With the Effelsberg 100-m telescope ($\delta S_\nu = 0.05$–0.35 Jy), searches were made of galaxies with large IR emission, galaxies exhibiting vibrational H_2 emission, and unusually active, radio-loud, or morphologically peculiar galaxies, independently detecting NGC 3079 (Henkel et al. 1984). Another survey of 43 bright ($S_{100\,\mu\mathrm{m}} > 50$ Jy, Dec $> -30^\circ$) *Infrared Astronomical Satellite* (IRAS) galaxies resulted in the detection of IC10 at 1 $L_\odot$ (Henkel, Wouterloot & Bally 1986). To establish the relationship of extragalactic masers with star formation activities, a high-sensitivity survey ($\delta S_\nu = 0.03$ Jy) of nuclei of nearby galaxies was carried out, detecting water masers from M 51 and NGC 253 (Ho et al. 1987). More recent surveys of IR galaxies have resulted in the detection of luminous maser sources in NGC 6240 and NGC 4051 (Hagiwara, Diamond & Miyoshi 2002, 2003; Nakai, Sato & Yamauchi 2002). In the Southern Hemisphere, the Parkes 64-m telescope was used to survey galaxies with declination south of -30° and heliocentric velocity below 1000 km s^{-1} ($\delta S_\nu = 0.5$ Jy). No new luminous maser was detected, aside from the known NGC 4945 and Circinus (Batchelor, Jauncey & Whiteoak 1982; Whiteoak & Gardner 1986).

In the last decade, all nearby galaxies with AGN characteristics were surveyed (Braatz, Wilson & Henkel 1996a, 1997), and from this work, it was recognized that luminous water masers are found primarily in galaxies with Seyfert2 and LINER[8] spectral characteristics. With the Nobeyama 45-m telescope and Parkes 64-m telescopes, a survey of nearby Seyfert1 and Seyfert2 galaxies was conducted, emphasizing the search for high velocity emission (Nakai et al. 1995). Since 1993, the NASA 70-m Goldstone antenna and the Parkes 64-m were used for extensive searches ($\delta S_\nu = 0.2$–0.5 Jy) of AGNs and star forming galaxies, with various characteristics including large far-infrared (FIR) flux, radio-excess, hard-X-ray emission with large absorbing columns, Seyfert2 or LINER spectra (Greenhill 1997, Greenhill et al. 2002). Recent searches with improved sensitivity ($\delta S_\nu = 0.02$ Jy) and a new spectrometer resulted in many new detections (Braatz et al. 2004, Greenhill et al. 2003a).

While most of the searches had been directed toward spiral galaxies, surveys of radio loud elliptical galaxies were also made. A survey of 50 FRI radio galaxies (radio loud ellipticals) was carried out (Henkel et al. 1998). Narrow absorption

[8]Low-ionization nebular emission region.

lines against symmetric radio sources may arise from circumnuclear torus and 8 out of 19 mega-masers show HI absorption (Taylor et al. 2002). However, no maser emission was detected out of five searched: Hydra A, PKS222-123, NGC3894, NGCC4151 and 0946+708, but the sensitivity of the search may not be enough to be conclusive. A survey of FRII radio galaxies with evidence of nuclear obscuration led to the detection of 3C 403 at $z = 0.06$ (Tarchi et al. 2003). An interesting search for a luminous H_2O maser from a gravitationally lensed quasar at $z \sim 2.6$ was made using the Australia Telescope Compact Array at 6 GHz, though without success (Wilner et al. 1999). A survey of Type II quasars has detected a giga-maser at $z = 0.66$, the most distant maser source known (Barvainis & Antonucci 2005).

Water mega-masers are rare. To date, there are more than 60 luminous water masers detected,[9] out of more than 1000 galaxies searched (Braatz 2002, Greenhill et al. 2002), but this number is bound to increase with time, given the increasing sensitivity of the searches (Braatz et al. 2004). Almost all the known water mega-masers are found in Seyfert2 or LINER nuclei, and there seems to be a trend for the mega-masers to be found in Seyfert2 galaxies exhibiting very-high-X-ray absorbing column ($N_H > 10^{24}$ cm^{-2}) (Braatz, Wilson & Henkel 1997; Greenhill et al. 2003a). More than a third of the mega-masers have compact radio cores, and 40% of Seyfert2 and LINERS have compact flat spectrum sources (Falcke et al. 2000). More than a third of the Seyfert2 galaxies searched host water mega-masers (Braatz et al. 2004).

6. TYPES OF H_2O MEGA-MASERS

Do all luminous nuclear H_2O masers, or H_2O mega-masers, originate from a circumnuclear disk as in NGC 4258? The answer requires VLBI mapping to delineate the structure and location of the maser emission sources. While the mega-masers may be luminous, their flux density is not always high enough for VLBI observations to be made. More than 10 known luminous H_2O masers have been mapped, but none as yet provides a comparably neat picture as NGC 4258. For example, in NGC 1068 and Circinus, the water mega-masers are associated with a rotating disk as well as shocked interstellar matter caused by a nuclear jet or wind. In NGC 1052 and Mrk 348, instead of being associated with a rotating disk, the maser emission is apparently located along a radio jet, at some distance (<1 pc) from the nucleus, presumably arising from postshocked gas as the nuclear radio jet impinges on the surrounding molecular clouds. Table 1 gives a few examples of the various types of nuclear H_2O mega-masers. A more detailed description of some of these sources is given in the following subsections.

[9]An up-to-date list of detected luminous water masers is maintained by J. Braatz at http://www.nrao.edu/∼jbraatz.

TABLE 1 Examples of different types of H_2O mega-masers

Galaxy	Spectral type	Distance (Mpc)	L_X (erg s^{-1})	Type	High-velocity emission (km s^{-1})
NGC 4258	Sy2	7.2	$10^{40.6}$	Disk	±900
IC 2560	Sy2	26	10^{41}	Disk	±<420
NGC 1068	Sy2	14.4	$10^{42.3}$	Disk+jet	± ≤350
Circinus	Sy2	4.2	$10^{42.3}$	Disk+outflow	±460
NGC 3079	Sy2	16	10^{41}	Disk+outflow?	± ≤225
NGC 1052	LINER	17	$10^{41.9}$–$10^{43.3}$	Jet	Broad
Mrk 348	Sy2	62.5	10^{43}	Jet	Broad
TX2226-184	LINER	102	—	?	Broad

6.1. Circumnuclear Masers

6.1.1. NGC 1068 NGC 1068, a proto-typical Seyfert2 galaxy, exhibits spectral lines from the broad-line region in polarized (reflected) light, which was taken to indicate the presence of an edge-on torus (Antonucci & Miller 1985). This putative nuclear torus was a part of the motivation for the suggestion that luminous water masers are circum nuclear instead of circum stellar (Claussen & Lo 1986). Thus, it is instructive to see if in fact the luminous water maser in NGC 1068 arises in a circumnuclear disk or torus.

The water maser emission in NGC 1068 ranges from $V_\odot \sim 800$–1500 km s^{-1}, with the systemic velocity of the galaxy at 1150 km s^{-1}. The bulk of the maser emission is from the presumed core of the compact radio source, S1 (Gallimore et al. 1996), except for the emission from ∼940–1040 km s^{-1} which is associated with component C of the radio source, 20 pc from S1. The association of water maser emission with a radio component that is many pc away from the presumed nucleus was the first indication that luminous nuclear water masers can also be associated with the nuclear outflow or jet, presumably originating in high-density gas that is being excited by the impact of the radio jet. Details of the physical conditions involved will be discussed below on the subject of jet-driven masers.

The maser emission from the nucleus S1 is distributed essentially linearly on the sky at a PA $\sim -45^\circ$ (Greenhill et al. 1996). The nuclear radio core S1 has been resolved into a pc scale roughly linear structure aligned at right angles to the local radio jet axis, and may trace thermal radio emission from a circumnuclear disk (Gallimore et al. 1996). However, the maser structure is not aligned with the major axis of S1 and thus also not at right angle to the radio jet (PA $\sim 0^\circ$). When plotted against the distance r from the nucleus, the velocity increases monotonically out to $r \sim 0.65$ pc, reaching a projected rotation velocity of 330 km s^{-1}, but decreases more slowly than $r^{-1/2}$ out to $r \sim 1.1$ pc. This suggests that the maser emission

originates from a rotating disk with a "sub-Keplerian" rotation curve, and the enclosed mass at 1.1 pc is $\geq 2 \times 10^7\ M_\odot$ (Greenhill & Gwinn 1997). A detailed analysis indicates that the "sub-Keplerian" rotation curve can be explained by taking into account the gravitational effect of the disk itself, suggesting that the mass of a possibly thick disk is almost comparable to the central mass (Hure 2002). Thus, in NGC 1068, the H_2O mega-maser emission is located in a circumnuclear disk or torus, with inner and outer radii of 0.65 pc and 1.1 pc, respectively, and also found in molecular clouds as a result of the impact of the radio jet.

6.1.2. CIRCINUS One of the nearest Seyfert2 galaxies at 4.2 Mpc, the Circinus galaxy has a bolometric luminosity of $\sim 4 \times 10^{43}$ erg s^{-1} and a L_X(2–10 keV) $\sim 2 \times 10^{42}$ erg s^{-1} with an absorbing column of 4×10^{24} cm^{-2}. An obscured broad-line region is evidenced by a polarized Hα line that is 3300 km s^{-1} wide, and there is a visible nuclear outflow on a kpc scale. *Hubble Space Telescope* (HST) observations show a complex of streamers and knots of high-excitation gas extending out of the galaxy. The morphology suggests that the high-excitation gas is concentrated on the surface of a hollow cone with a V-shaped apex close to the nucleus that may result through entrainment of dense gas from a circumnuclear torus by a low-density, outflowing wind or jet (Wilson et al. 2000, Ruiz et al. 2001).

The luminous water maser in Circinus was among the first discovered (Gardner & Whiteoak 1982), and only relatively recently that maser emission blueshifted relatively to the systemic velocity was discovered (Nakai et al. 1995; Braatz, Wilson & Henkel 1996). The maser emission from Circinus was observed to be extremely time variable, on time scales as short as a few minutes. The most plausible explanation of such variability may be the result of strong interstellar diffractive scintillation, which places stringent upper limits of 1–10 AU on the apparent sizes of the maser components, implying very large brightness temperature, $>10^{16}$ K (Greenhill et al. 1997).

Recent VLBI observations of the Circinus water maser source made with the Australia Telescope Long Baseline Array (Greenhill et al. 2003b) show that the maser emission is distributed along a thin, densely sampled, S-shaped locus that comprises redshifted emission to the west and blueshifted emission to the east. The arms of the S exhibit velocity gradients along their lengths with increasingly large Doppler shifts toward the center. Most of the remainder of the maser emission, occupying the central $\sim$260 km s^{-1} of the spectrum, comprises knots that lie outside the S and away from the putative disk. The spatial distribution of the maser emission is summarized in Figure 5. The maser emission from close to the S-shaped locus (amounting to $\sim$40% of the integrated emission) falls closely on the Keplerian rotation curve.

Thus, the maser emission appears to trace an edge-on warped disk between the radii of 0.1 pc and 0.4 pc, as well as a wide-angle outflow that extends up to $\sim$1 pc from the estimated disk center. The maximum rotation velocity of the disk is 260 km s^{-1} and the inferred enclosed mass within 0.1 pc is $\sim 1.7 \times 10^6\ M_\odot$. Very recently, extremely high-velocity emission up to ± 460 km s^{-1} from the systemic

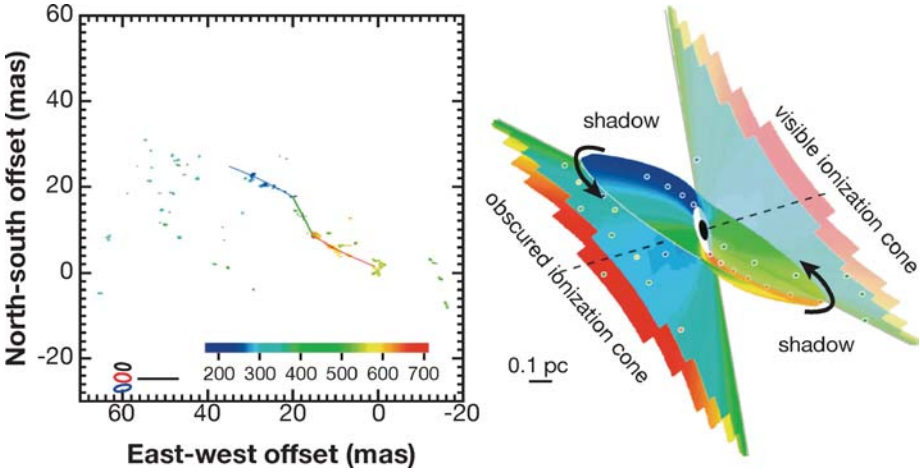

Figure 5 Circinus: The *left panel* (*a*) shows the spatial distribution of the maser emission; the *right panel* (*b*) shows a model of the source of the maser emission from a warped disk and an outflow from the center (Greenhill et al. 2003b).

velocity has been discovered. If this emission arises from the Keplerian accretion disk, it lies at 0.03 pc radius, which would imply a very high central stellar density of $\sim 6 \times 10^{10} M_{\odot}/\mathrm{pc}^3$ (Greenhill et al. 2003a), higher than that of NGC 4258 and the galactic center.

6.1.3. NGC 3079 One of the first luminous nuclear water masers detected, NGC 3079, is an edge-on SBc galaxy with strong water emission in a range of velocity that is blueshifted from the systemic velocity (Henkel et al. 1984, Haschick & Bann 1985). Redshifted emission features were discovered later (Trotter et al. 1984, Hagiwara et al. 2002). The nuclear region exhibits OH absorption at the systemic velocity (Haschick & Baan 1985), HI absorption against the nuclear radio continuum source (Sawada-Satoh et al. 2000) and CO emission that is distributed over ~500 pc (Koda et al. 2002).

An early 4-station VLBI experiment revealed that the individual water spectral features were unresolved and smaller than 1.5×10^{16} cm, with $T_{\mathrm{b}} > 4 \times 10^{12}$K, coincident with the radio continuum source to within 5 mas. This coincidence was used to argue for amplification by a foreground cloud, 50 pc from the background radio source and associated with a massive star or shocked molecular region (Haschick et al. 1990). Subsequent, more detailed VLBI mapping showed that the continuum source is composed of three colinear components, presumed to be a part of a core-jet structure. Most of the maser emission is in a clump ~0.05 pc in size, 0.5 pc offset from the nearest compact radio component, implying that the large apparent luminosity is not caused by beamed amplification of high brightness radio continuum. The rest of the maser emission is spread over ~2 pc. A couple of

faint features lie along the radio continuum axis, with the balance of the emission aligned at an angle to the radio axis.

The distribution could be cast in a model of a tilted rotating molecular disk where the bulk of maser emission arises, with a radio jet emanating at an angle from the center of the jet. Faint maser emission associated with a faint radio continuum feature along the radio continuum axis suggests a second population of maser emission that is associated with jet driven gas (Trotter et al. 1998, Yamauchi et al. 2004, Kondratko et al. 2005). Phase reference measurements relative to the bright maser features indicate that one of the radio component has a proper motion, while the maser features show no measurable proper motion (Sawada-Satoh et al. 2000).

6.2. Kinematic Evidence for Circumnuclear Disk

In the case of NGC 4258, a strong evidence for an edge-on rotating accretion disk was the centripetal acceleration of the maser emission orbiting in front of the nucleus (Figure 3). Hence, a change of the velocity of a spectral feature may be taken as evidence for the maser source in a rotating accretion disk, even though to detect the velocity change of the systemic features requires regular observations over a long period. Besides NGC 4258, acceleration has been found in NGC 2639 at 6.6 ± 0.4 km s^{-1} year^{-1} (Wilson, Braatz & Henkel 1995), IC 2560 at 2.62 ± 0.09 km s^{-1} year^{-1} (Ishihara et al. 2001), and possibly NGC 2960 at 2.8 ± 0.5 km s^{-1} year^{-1} (Henkel et al. 2002). In addition, the spectra of water maser emission from IC 2560 and NGC 2960 both have high-velocity features offset from the systemic velocity by up to $\sim$350 km s^{-1} and $\sim$500 km s^{-1}, respectively. Monitoring of the high-velocity feature showed no detectable velocity change ($<$1 km s^{-1} year^{-1}) in either case, which is expected in the rotating disk model.

6.3. Nuclear Jet Driven Masers

6.3.1. NGC 1052 In NGC 1068, a part of the luminous water maser emission is associated with a component of the nuclear radio source 20 pc from the nucleus. This association of a luminous water maser with the radio jet, and not the active galactic nucleus itself, is even clearer in the case of NGC 1052, an elliptical galaxy with LINER characteristics. VLBA observations showed that the nuclear radio source in NGC 1052 has a complicated linear structure with at least seven components (Claussen et al. 1998, Kameno et al. 2003). The maser emission, redshifted by 100–150 km s^{-1} from the systemic velocity of the galaxy, instead of being aligned perpendicular to the radio jet as one would expect in the case of an accretion disk maser is aligned along the radio jet closely following the ridge line of the radio brightness distribution (Figure 6). The maser emission is distributed over $\sim$0.05 pc, in two groups whose centroids are $\sim$0.08 pc apart, with a distinct velocity gradient along the jet (Claussen et al. 1998). If the true nucleus is at a gap of the 22 GHz radio continuum, due to foreground free–free absorption by

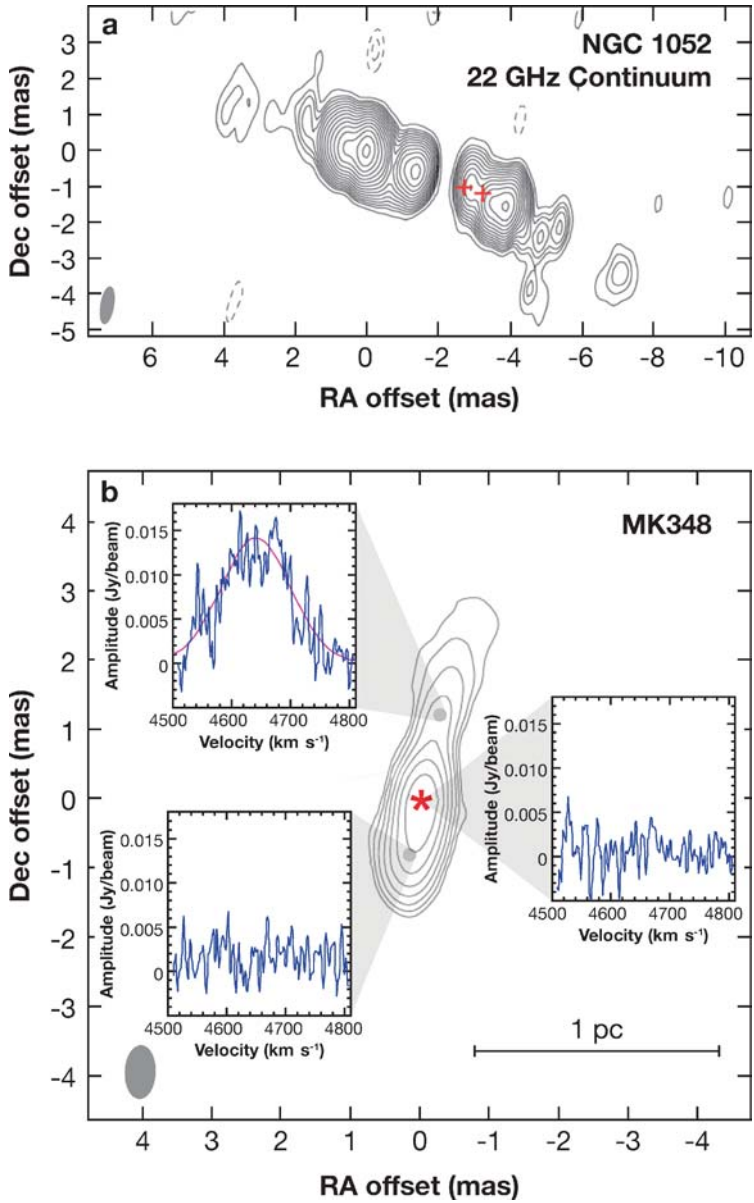

Figure 6 The *top panel* (*a*) shows the distribution of water maser emission along the radio continuum ridge in NGC 1052, and the *crosses* mark the positions of the maser emission (Claussen et al. 1998); and the *bottom panel* (*b*) shows the VLBI map of the 22 GHz (λ1.3 cm) nuclear radio continuum emission from Mrk 348 (*contours*) and the spectra are those of the maser emission from the positions indicated by the *gray dots* and *asterisk*. The *asterisk* marks the presumed position of the galactic nucleus (Peck et al. 2003).

cold dense plasma in a circumnuclear torus (Kameno et al. 2003), then the maser emission originates at a distance $\geq \sim 0.2$ pc from the center.[10]

To account for Galactic masers, it has been suggested that jets, winds or outflows interacting with the interstellar medium can produce the conditions suitable for maser emission. The high-pressure region produced by a jet impinging on the surrounding medium drives a radiative shock ahead of it, compressing and heating the postshock material to produce the requisite conditions for maser emission, such as raising the kinetic temperature of the gas and enhancing the gas phase H_2O abundance (Elitzur et al. 1989, MacLow et al. 1994). Evidently, in NGC 1052, the radio jet is energetically capable of powering the maser emission by driving slow, nondissociative shocks into the surrounding dense molecular clouds. The broad-line profile of the maser emission in NGC 1052 showed significant changes over a period of 1.5 years with the peak velocity increasing by ~ 75 km s^{-1} (Braatz et al. 2003). Proper motion studies of the maser emission would help to understand in more detail the relationship of the masers and the jet.

6.3.2. Mrk 348 Another example of jet-driven H_2O mega-masers is Mrk 348 (Falcke et al. 2000). Mrk 348 is a nearly face-on early-type spiral, with a Seyfert2 nucleus, UV excess, and a bright and variable radio nucleus (Ulvestad et al. 1999). The galaxy also has a large HI halo with tails, indicating probable interaction with NGC 2266. The mega-maser emission from Mrk 348 is very broad in linewidth 130 km s^{-1}, and redshifted from the systemic velocity of the galaxy. All the maser emissions are found to coincide with a radio jet at ~ 0.3 pc from the radio core, but unresolved by a beam of 0.5 mas, which puts an upper limit to the total maser extent of <0.25 pc (Figure 6). The higher velocity emission may rise closer to the nucleus, and delays in the variability across the line profile imply a spatial extent of the maser emission of ~ 0.07 pc or 2×10^{17} cm. Furthermore, the correlation of the variations in the maser flux and the radio continuum flux may be consistent with the idea that both increases are due to the ejection of new radio components (Peck et al. 2003). Thus, similar to NGC 1052, the maser in Mrk 348 is physically associated with the nuclear jet.

With sufficient resolution, the maser emission in Mrk 348 can be resolved and used to probe the velocity structure of the postshock gas in which the maser emission arises. Spatially resolved observations and proper motion studies of the maser emission simultaneously with the radio continuum core and jet would be very powerful analytical tools for both the excitation mechanism of the maser, the structure of the postshock gas, and the radio source itself. Detectability of jet-driven masers may be optimized by jets in the plane of the sky inducing radiative

[10]It has been argued that the nucleus is actually in the brightest radio continuum peak where the maser emission arises and therefore the masers could be circumnuclear disk (Sawada-Satoh et al. 2005). On the other hand, analysis of multi-wavelength observations suggest that the nucleus is at the gap (Vermeulen et al. 2003). Further observations are needed to settle where the nucleus of NGC 1052 is.

shocks whose front is more aligned along the line of sight (Peck et al. 2003). As there are relatively few nearby radio galaxies, the observed flux density may tend to be lower and requires higher sensitivity observations compared to the Seyfert and LINER samples.

The spectra of the jet-driven maser emission from both the NGC 1052 and Mrk 348 are composed of one broad continuous component, instead of many narrow components seen in most water maser emission spectra. This raises the question whether this spectral characteristic implies the jet-driven origin of the maser emission. Other galaxies with broad spectral shapes include TXS2226-184 (Koekemoer et al. 1995), NGC 2824, and F01063-8034 (Greenhill et al. 2003a).

6.4. Nuclear Kilo-Masers

Extragalactic water masers with a luminosity up to a few $L_{\odot}$, comparable to or slightly larger than the most luminous of Galactic water masers, are sometimes termed "kilo-masers." The question is whether the kilo-masers found in galactic nuclei, such as those in M 51 (Ho et al. 1987), NGC 253 (Ho et al. 1987, Nakai et al. 1988, Henkel et al. 2004), M 82 (Claussen, Heiligman & Lo 1984; Henkel et al. 1984), and NGC 2146 (Tarchi et al. 2002a), are associated with the AGN or stars. In nuclear regions where there is enhanced star formation or a starburst, a large number of interstellar masers can be expected near young stellar objects, and masers with large luminosity are expected statistically (Ho et al. 1987). Most nuclear kilo-masers are likely physically associated with star formation, and the clearest case is M 82 (Baudry & Brouillet 1996). However, such galaxies could also harbor an AGN, and the "kilo-maser" could be a weak version of circumnuclear masers, which could be the case for M 51 (Hagiwara et al. 2001). While mega-masers cannot be powered by stars, kilo-masers can be powered by either stars or AGN, so that the term is not a good indicator of the physical origin of the masers.

7. CIRCUMNUCLEAR MOLECULAR GAS AND H_2O MASER EMISSION

The classification of AGNs, such as quasars and Seyfert nuclei, is based on the spectral lines from ionized gas within tens of pc of the center. The existence of molecular gas under the conditions near active galactic nuclei was anticipated as one of the thermally stable phases (Lepp et al. 1985). This has been indirectly confirmed by the inferred presence of obscuring dust, and thus high-density gas, in the form of circumnuclear tori at the pc scale, from spectro-polarimetric observations (Antonucci & Miller 1985). The direct detection of abundant molecular gas in nuclear regions has been made via the detection of millimeter-wave CO lines, but on the 100-pc to kpc scale (e.g., Schinnerer et al. 2000). In our own Galactic

center, molecular gas is found in a circumnuclear disk with an inner edge at a radius of ∼1 pc, surrounding a central region of atomic and ionized gas (Morris & Serabyn 1996). Luminous H_2O masers are located very close to active galactic nuclei, in molecular accretion disks and the associated outflow within the central pc, or in the molecular gas excited by radio jets within tens of pc of the center. These mega-masers constitute direct evidence for high-density molecular gas very close to the AGN.

The physical conditions of molecular clouds in circumnuclear disks or tori are controlled by the large X-ray flux found in the AGN (Krolik & Kallman 1983, Lepp & McCray 1983, Krolik & Lepp 1989, Draine & Woods 1991). Under a wide range of X-ray fluxes and gas pressures in a molecular accretion disk, X-ray heating can give rise to warm neutral gas with a large water abundance, leading naturally to collisionally pumped water maser emission with sufficient power to account for the luminous masers (Neufeld, Maloney & Conger 1994). Because of the penetrating power of hard X-rays ($E \geq 1$ keV), the X-ray-dominated region (XDR) extends over a large column density and its properties vary slowly with depth (Maloney et al. 1996), which would create a larger volume of masering medium compared to FUV heating of molecular gas by stars as in the case of the Galactic PDRs. As the observed flux density is highly dependent on the gain length of the maser source, a larger volume of the masering medium would be more favorable to the production of luminous maser emission.

However, in a medium with a large column density, far infrared (FIR) photons trapped by the water molecules can quench the population inversion. When the presence of cold dust in the gas is taken into account, it was shown that these FIR photons are absorbed, allowing for a much larger extent in which population inversion is not quenched and remains constant with increasing optical depth, thereby accounting for the large luminosity observed in water mega-masers (Collison & Watson 1995). Dust grains with a temperature lower than the gas temperature are required, but this is expected in the X-ray-heated disk (Desch et al. 1998). Other submillimeter water transitions under the same physical setting could also have maser luminosity comparable to the 22 GHz transition (Wallin & Watson 1997), and they could be observable as the appropriate instrumentation becomes available.

Besides X-ray irradiation, heating of the gas to pump the maser can also be due to shock waves within the disk and viscous heating. Since viscous dissipation must exist in an accretion disk, one can examine if viscous heating is sufficient to maintain the physical conditions for maser emission, i.e., a gas temperature of 300–400 K, densities of 10^7–10^{10} cm^{-3}, and a dust temperature 50–100 K below the gas temperature. From considerations of the cooling rate of the accretion disk under such conditions, it was concluded that if the viscous dissipation of heat with distance from the mid-plane of the disk is quite different from the distribution of mass, viscous heating cannot be ignored (Desch et al. 1998). This suggests that X-ray irradiation may not be the only heating mechanism for luminous water masers.

It was also proposed that the maser emission in NGC 4258 arises within thin slabs of postshock gas from a spiral shock in the circumnuclear disk. This mechanism can naturally account for the dominance of the redshifted high-velocity emission over the blueshifted high-velocity emission (Maoz & McKee 1998). However, the predicted velocity shift of the high-velocity emission in this model has not been verified by observations (Bragg et al. 2000).

The spectra of luminous water masers typically consist of narrow features, each a few km s^{-1} wide within a range of velocity, covering one to a few $\times 100$ km s^{-1}. Each feature can vary, or disappear completely, but new features can appear at different velocities, on the time scale of days to months. This property is quite similar to that of Galactic interstellar masers, for which it has been proposed that variations can be due to changing alignment along the line of sight of two maser clumps within the maser source (Deguchi & Watson 1989). Along similar lines, the implications of a clumpy circumnuclear disk on the spectra and variability of luminous water maser emission have been investigated (Kartje, Königle & Elitzer 1999). Alternately, irregularities in the velocity field, or turbulent motion, in the circumnuclear disk can also lead to spectra similar to what is observed (Wallin, Watson & Wyld 1998, 1999).

Correlated variability of the maser intensity in the blue and redshifted features was observed in NGC 1068, implying that the maser emission is responding to the central exciting source (Gallimore et al. 2001). The mechanism of this coordinated variation is probably due to changes in the central source of the X-ray luminosity (which controls the heating rate) or of the bolometric luminosity (which changes the temperature difference of the gas and dust) in the maser region. Both changes will affect the population inversion of the molecules and therefore the maser output (Neufeld 2000).

In Circinus, it appears that maser emission is also associated with the nuclear outflow in addition to the circumnuclear disk. Centrifugally driven winds from the surfaces of magnetized accretion disks may provide the mechanism for producing bipolar outflows and jets. In the outer regions of the disk, neutral gas and dust could be lifted above the disk without being ionized or destroyed by the radiation from the central source (Kartje, Königl & Elitzur 1999; Königl & Kartje 1994). In the case of NGC 1068 and Mrk 348 where the maser emission coincides with a radio jet, it is more likely that the maser emission arises in the postshocked gas as the nuclear outflow or wind impacts the surrounding molecular clouds. For such jet-driven luminous masers, there has been no detailed study of the conditions specific to a nuclear radio jet, but studies of the general conditions applicable to Galactic masers are likely to be relevant.

In summary, H_2O mega-masers originate in dense molecular gas within parsecs of an AGN, either in an accretion disk heated directly by radiation from the AGN, or in circumnuclear molecular clouds excited by the impact of a jet or an outflow from the AGN. They are very useful high-resolution probes of high-density molecular gas in the vicinity of an AGN, which is otherwise difficult to observe directly.

8. OH MEGA-MASERS

8.1. Discovery and Early Surveys

Unlike the λ1.35 cm H_2O line, the λ18 cm OH lines originate from the ground state so that given a limited sensitivity, absorption against a radio continuum source provides an effective way of detecting extragalactic OH. Thus, extragalactic OH was initially detected in absorption in the edge-on spiral galaxy NGC 253 and the irregular galaxy M 82 (Weliachew 1971). With improved sensitivity and spectral resolution, weak 1667 MHz OH emission with a narrow linewidth ($\sim$10 km s^{-1}), in addition to the OH absorption, was seen in NGC 253 (Whiteoak & Gardner 1973, Gardner & Whiteoak 1975) and in M 82 (Rieu et al. 1976). In contrast to bright Galactic OH masers, the OH emission from both galaxies is more than 10 times stronger and unpolarized, and the 1667 MHz line is stronger than 1665 MHz. For both galaxies, it was proposed that foreground maser amplification of the background radio continuum is needed to account for the unusually bright maser emission (Whiteoak & Gardner 1973, Rieu et al. 1976).

In the course of a survey for OH absorption in galaxies with known HI absorption, very intense and broad (full width at zero intensity (FWZI) of $\sim$400 km s^{-1}) OH emission was discovered from the peculiar galaxy IC 4553 (Arp 220) with the Arecibo telescope (Baan, Woood & Haschick 1982). The isotropic luminosity of this emission (1.4×10^{36} erg s^{-1} $\sim$ 400 $L_\odot$) equals $\sim 10^8$ times that of W3(OH), a typical Galactic interstellar OH maser source (Figure 2). However, unlike Galactic sources such as W3(OH), the emission is unpolarized and the 1667 MHz line is stronger than the 1665 MHz line. While these properties are similar to those of the OH emission from NGC 253 and M 82 described above, but the OH emission linewidth is exceptionally large (FWZI $\sim$ 400 km s^{-1}). If the emissions were thermal, then the mass of OH molecules alone would be $7.5 \times 10^7 M_\odot$. The anomalously strong OH emission could also be due to a large number of OH maser sources associated with HII regions (Baan, Wood & Haschick 1982). Subsequent observations with 0.3″ resolution showed that $T_b > 10^6$ K, thus ruling out the thermal origin of the emission (Norris 1985).

After the detection of the unexpectedly strong OH emission in IC 4553 (Arp 220), surveys for OH mega-masers were conducted on all the telescopes with significant collecting area, such as the Arecibo 305-m telescope, the NRAO 91-m telescope, the Jodrell Bank MkIA 76-m telescope, the Nancay 300-m telescope, and the Parkes 64-m telescope in the Southern Hemisphere. Under the model of OH mega-maser emission to be foreground amplification of background radio continuum sources, searches were conducted of galaxies with HI absorption, strong radio continuum and IR sources, and Markarian and IRAS galaxies (Baan et al. 1985, Schmelz et al. 1986). Initially, the detection rate of OH mega-masers was very low, amounting to 3 out of 240 galaxies searched (Baan, Schmelz & Haschick 1985).

The association of OH mega-masers and starburst activities was proposed, since the environments for starbursts could provide the conditions favorable to maser

emission, such as a strong IR radiation field, high-density gas, and the presence of radio continuum sources (Bottinelli et al. 1985). It was then noted that the known OH mega-masers have IR colors that indicate strong excesses at both 25 μm and 60 μm (Henkel, Wouterloot & Bally 1986; Unger et al. 1986), which led to surveys of IRAS galaxies with the appropriate color (Staveley-Smith 1987, 1992; Norris et al. 1989). Other surveys of IRAS galaxies selected on the basis of large IR to blue ratio (Bottinelli et al. 1985) or the high-FIR luminosity ($>2 \times 10^{10}\ L_{\odot}$) (Mirabel & Sanders 1987) were also carried out. A search was made of the FIR-luminous radio galaxy 4C 12.50 with a tentative detection (Dickey et al. 1990).

8.2. Probes of Distant Galaxies

Given that most types of OH population inversion require FIR pumping, the ratio $L_{\rm OH}/L_{\rm FIR}$ provides a measure of the pumping efficiency. It was noticed that this ratio is larger in the most luminous IR galaxies, and the analysis of 16 OH mega-masers led to the relationship, $L_{\rm OH} \propto L_{\rm FIR}^2$ (Martin et al. 1988, Baan 1989). In the context of foreground amplification of background radio continuum, this quadratic relationship may be expected, if the population inversion is pumped by the FIR radiation field and the radio continuum (which itself is proportional to the FIR luminosity) is being amplified by an unsaturated maser cloud (Baan 1989). However, when the likely difference in the size scales of the FIR and the OH mega-maser sources is taken into account, the reliability of deducing the underlying physical mechanisms based on such global measures should be treated with caution.

The quadratic relationship, $L_{\rm OH} \propto L_{\rm FIR}^2$, implies that galaxies with $L_{\rm FIR} \geq 10^{13} L_{\odot}$ (hyperluminous IR galaxies, HLIRGs (Rowan-Robinson 2000)) could reach OH luminosity in the range of 10^5–$10^6\ L_{\odot}$. In fact, the so-called "giga-masers" with $L_{\rm OH} \geq 10^4\ L_{\odot}$ do exist: IRAS 20100-4156 at $z = 0.129$ (Staveley-Smith et al. 1989), IRAS 14070+0525 at $z = 0.265$ (Baan et al. 1992), and IRAS 12032+1707 at $z = 0.217$, all with $L_{\rm FIR} \sim 2 \times 10^{12}\ L_{\odot}$ (Darling & Giovanelli 2001). The possibility of such a large OH luminosity raised the prospect of OH mega-masers being detected at very high z (Burdiuzha & Komberg 1990). If the OH mega-masers preferentially trace the high-luminosity IR galaxies which tend to be galaxy mergers, it was suggested that a blind radio spectroscopic survey at frequencies of 400–1000 MHz can form an independent test of the galaxy merger rate as a function of time over the redshift interval z = 4–0.7 (Briggs 1998).

Recent discovery of distant submillimeter (submm) galaxies has uncovered a population of young galaxies via their redshifted rest-frame FIR energy from starbursts embedded in dusty regions that may make significant contribution to the star formation at $z > 1$. However, the redshift distribution of such galaxies is required to derive the history of obscured star formation (Blain et al. 2002). As the submm galaxies are faint in optical and infra-red (OIR) by definition, OIR redshift determination has been difficult. By applying the radio-IR photometric method (Carilli & Yun 1999), it has been demonstrated that submm galaxies are

distant objects as their median redshift is $2 < z < 3.5$ (Carilli & Yun 2000). The possibility of using OH (and H_2O) mega-maser emission from submm galaxies to determine the redshift distribution of luminous, dust-enshrouded, star forming galaxies has been pointed out. If OH mega-maser luminosities could reach the level of $\geq 10^5\ L_\odot$, the observed flux densities would be of the order of 1 mJy and can be detected with current instrumentation out to $z \approx 4$. The advantage of this approach in determining redshift from submm galaxies is that the bandwidth of the required spectrometer is <1 GHz and technically achievable (Townsend et al. 2001).

8.3. Upgraded Arecibo Survey

After an upgrade, the sensitivity of the Arecibo 305-m telescope improved fivefold since the first detection of OH mega-maser emission in IC 4553, and an extensive search for OH mega-masers was undertaken (Darling & Giovanelli 2000, 2001, 2002a). By then, it was known that all OH mega-masers were found in luminous IR galaxies, with the OH luminosity increasing quadratically with IR luminosity. The survey galaxies were selected from the IRAS Point Source Catalog Redshift Survey (PSCz) (Saunders et al. 2000), with $f_{60\,\mu\mathrm{m}} > 0.6$ Jy, falling within the Arecibo declination range of $0^\circ < \delta < 37^\circ$ and the redshift range of $0.1 < z < 0.45$. In practice, radio-frequency interference limits the search to $z < 0.23$ ($\nu < 1355$ MHz). Given the flux limit and $z > 0.1$, the sample galaxies have $L_{\mathrm{FIR}} \geq 10^{11.4}\ L_\odot$ and are primarily luminous IR galaxies (LIRGs). The sample includes 311 galaxies, observed in 200 h on the 305-m telescope with an instantaneous bandwidth covering $\sim$4500 km s^{-1}. The survey resulted in the detection of 52 OH mega-masers, 1 OH absorber, and 25 ambiguous cases due to Galactic HI or man-made interference. The overall detection rate is 1 in 5.5, but it is a strong function of L_{FIR}, increasing to >1/3 for ULIRGs with $L_{\mathrm{FIR}} \geq 10^{12}\ L_\odot$. There is also a tendency for the LIRGs with OH mega-masers to have warmer FIR colors (smaller $f_{100\,\mu\mathrm{m}}/f_{60\,\mu\mathrm{m}}$) (Figure 7).

From a combined sample of 95 OH mega-masers, and after accounting for the Malmquist bias,[11] it was found that instead of the quadratic relationship between the OH and FIR luminosities, $L_{\mathrm{OH}} \propto L_{\mathrm{FIR}}^{1.2\pm0.1}$ (Darling & Giovanelli 2002a). The scatter about this mean relationship is considerable, however. Since the FIR emission and OH mega-maser emission almost certainly do not all originate from the same physical locations, scatter in the correlations of such global quantities is expected. Furthermore, it is important to remember that while this relationship is intriguing and suggestive for the IR luminous galaxies with detected OH emission, a large fraction of the IR luminous galaxies do not exhibit OH mega-maser emission at all. This indicates that other factors besides IR luminosity are necessary for the production of OH mega-maser emission.

[11]This bias refers to the fact that in sensitivity-limited surveys, the detection of the more distant sources tends to favor the bright end of the luminosity distribution of sources.

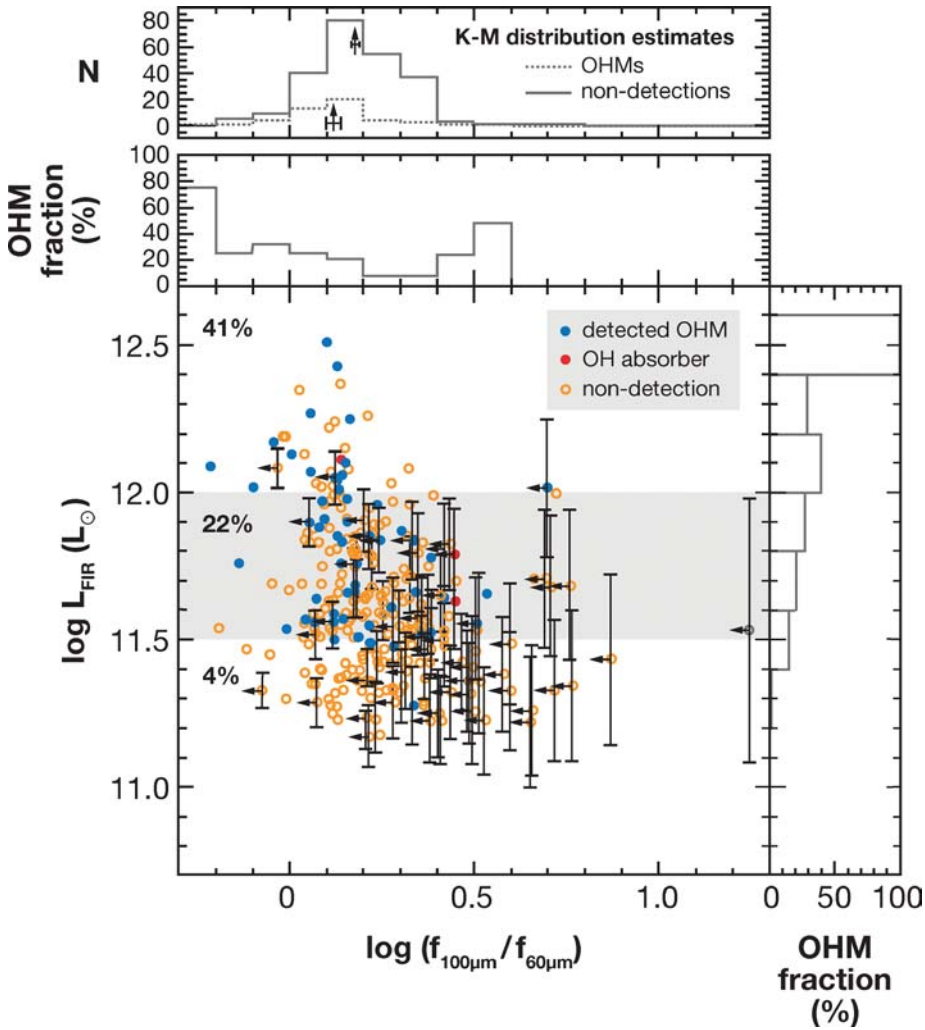

Figure 7 The large *central diagram* is a plot of the FIR color (*horizontal axis*) versus the FIR luminosity (*vertical axis*) of the LIRGs surveyed for OH mega-maser (OHM) emission. The *top two diagrams* show that the LIRGs with OH mega-maser emission tend to have warmer FIR colors. The *diagram on the right* suggests that OH mega-maser emission is more common among more luminous LIRGs. See also the % OH mega-maser detection rates of the LIRGs in three different luminosity ranges indicated on the *left of the central diagram* (Darling & Giovanelli 2002a).

It was found that the LIRGs with OH mega-maser emission appear to be more IR luminous or radio deficient, compared to LIRGs with OH nondetections. This could be due to the OH host LIRGs undergoing very recent star formation in which the overall radio continuum emission has not yet caught up, delayed by at least the lifetime of the massive stars that end as supernovae. The most luminous OH mega-maser is not only strong, but has a large linewidth at 10% peak intensity, and the two most luminous OH mega-masers have multiple line components (Darling & Giovanelli 2002a).

Based on a large sample and $L_{\rm OH} \propto L_{\rm FIR}^{1.2}$, an OH mega-maser luminosity function has been constructed: $\Phi \propto L_{\rm OH}^{-0.64}\,{\rm Mpc}^{-3}\,{\rm dex}^{-1}$, which is well determined for $10^{2.2}\,L_\odot < L_{\rm OH} < 10^{3.8}\,L_\odot$ and $0.1 < z < 0.23$ (Darling & Giovanelli 2002c). Up to dozens of OH mega-masers may be detected per square degree per 50 MHz by a survey reaching an rms noise of 100 μJy per 0.1 MHz channel. Arecibo already reaches 200 μJy in a 0.05 MHz channel with 4 min on source.

9. HIGH-RESOLUTION STUDIES OF OH MEGA-MASERS

While surveys have shown that OH mega-masers tend to be found in IR luminous galaxies with the warmest IR colors, 80% of the LIRGs surveyed are not OH mega-masers. From the analysis of 31 OH mega-masers, it was argued that the OH mega-maser properties can be accounted for based on three conditions: (1) the emission is due to the amplification of an intense radio continuum background; (2) the excitation temperatures for the main lines are equal, and (3) the ratio of optical depths is consistent with the LTE value (Henkel & Wilson 1990). However, many issues remain, such as the extent and conditions of the amplifying cloud, the distance between the cloud and the background radio continuum source, their relationship to other components such as starbursts or AGN in the host galaxies, and the reasons why 80% of the IR luminous galaxies do not exhibit OH mega-maser emission. To address the issues, high-resolution observations are necessary to help identify the detailed conditions for forming OH mega-maser emission. Because of the weakness of OH mega-maser emission and the large distances, only a few OH mega-masers have been studied in detail so far.

With a resolution of $\sim 1''$ in the A configuration, the VLA was used to study the OH mega-maser sources at a linear resolution of $\geq$200 pc: in IC 4553 (Arp 220) (Baan & Haschick 1984), Mrk 273 (Schmelz, Baan & Haschick 1987), Arp 299 (IC 694 and NGC 3690) (Baan & Haschick 1990), IRAS 17208-0014 (Martin et al. 1989), and III Zw 35 (Montgomery & Cohen 1992). At this resolution, the OH mega-maser emission was found to coincide with the radio continuum very closely and to be typically $\leq 1''$ or a few hundred pc, as in Arp 220 and IRAS 17208-0014. This coincidence was taken as evidence for supporting the model of foreground clouds amplifying background continuum as OH mega-maser emission (Baan & Haschick 1984, Martin et al. 1989). However, in the cases where the radio continuum is resolved into multi-components, the OH emission was often found

to correspond to only one of the components, usually the one with the brightest IR emission, as in Mrk 273, Arp 299, and III Zw 35.

9.1. Arp 220

IC 4553 was the first OH mega-maser detected. With the advent of the IRAS satellite, IC 4553 was found to have a very large FIR luminosity of $1.4 \times 10^{12}\ L_{\odot}$ and came to be known better as Arp 220, a galaxy merger as evidenced by tidal tails. MERLIN[12] observations at $\sim 0.2''$ resolution show that the radio continuum emission is extended over the central $\sim$1 kpc, with two peaks coincident with the two IR nuclei $\sim 1''$ (370 pc) apart (Graham et al. 1990; Mundell, Ferruit & Pedlar 2001). Both radio continuum peaks are extended by $\sim$100 pc. The OH mega-maser emission has three extended components. One is found to coincide with the eastern radio continuum peak, and the other two to bracket the western radio continuum peak to the north and south (Rovilos et al. 2003).

Observations of CO emission at a resolution of $\sim 0.5''$ from Arp 220 have shown that there is a central kpc-scale molecular gas disk, embedded in which are two nuclear disks, each containing $\sim 10^9\ M_{\odot}$ of molecular gas, within 100 pc of each of the two nuclei (Downes & Solomon 1998, Sakamoto et al. 1999). The close similarity of both the spatial distributions and the velocity fields of the OH mega-maser emission and of the CO(2–1) emission suggests that the OH mega-maser emission in Arp 220 originates from the two nuclear molecular disks (Figure 8). In particular, the similarity of the velocity fields of the OH and CO emissions is difficult to explain if the OH emission arises in a foreground amplifying cloud unrelated to the nuclear molecular disks.

To study the internal structure of the OH mega-maser sources below the 100-pc scale, VLBI observations that provide pc-scale resolution are required. The model of dense gas in the inner few hundred pc of the OH mega-maser galaxies amplifying background radio continuum from the nuclear regions has been commonly accepted. So the discovery that most ($\sim$70%) of the OH mega-maser emission from Arp 220 originates in structures $\leq$10 pc and aligned with a weak but compact radio continuum structure came as a surprise, as the observations imply that the OH mega-maser emission originates very close to the galactic nucleus (Lonsdale, Diamond & Smith 1994).

More complete global VLBI observations of Arp 220 (at 3 mas $\times$ 8 mas or 1 pc $\times$ 2.5 pc resolution) showed that 2/3 of the OH maser emission originate from four compact regions, typically 10–20 pc size, two in each of the two nuclei. Two of the compact sources are elongated, $\sim$30 pc $\times$ 1 pc (Lonsdale et al. 1998). The same observations also showed that embedded in the extended radio continuum emission are $\sim$12 unresolved sources spread over a 75 pc $\times$ 150 pc region in the NW nuclear region and 1–2 unresolved sources in the SE nucleus. These sources are

[12]Multi-Element Radio Linked Interferometer Network (MERLIN), operated by Jodrell Bank Observatory.

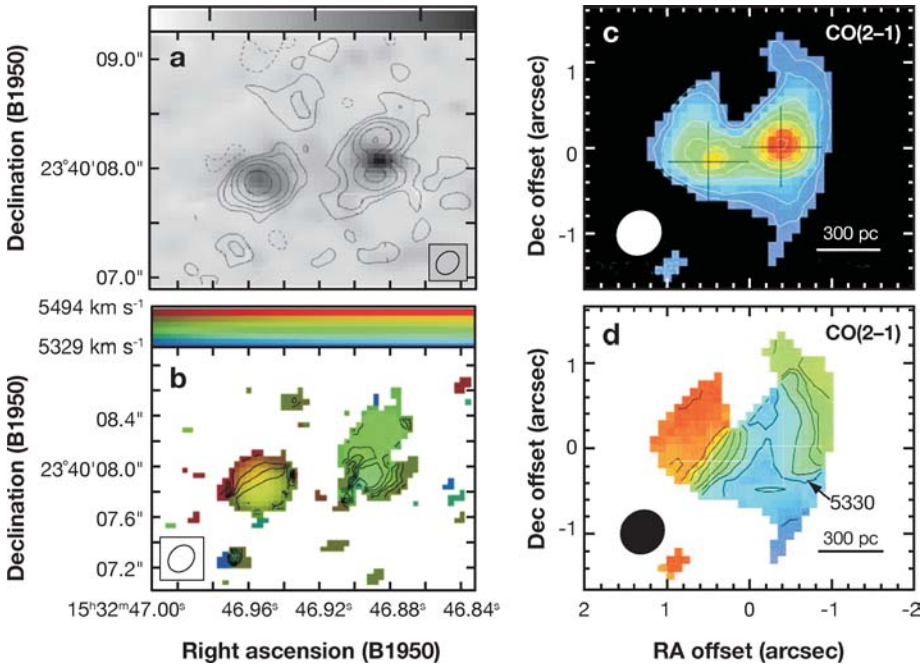

Figure 8 Arp 220: the *left panels* show the spatial distribution and velocity field (*contours* spaced by 10 km s^{-1}) of the OH mega-maser emission (Rovilos et al. 2003); the *right panels* show the spatial distribution and velocity field (*contours* spaced by 50 km s^{-1}) of CO(2–1) emission (Sakamoto et al. 1999). The spatial scales of the figures are similar but not identical. The similarity of the velocity fields strongly suggests that the OH mega-maser emission originates from the extreme starburst region at the galactic nuclei of Arp 220 and not in some foreground clouds.

most likely luminous radio supernovae, consistent with a starburst at the rate of 50–100 $M_\odot$ $year^{-1}$ needed to account for the observed FIR luminosity (Smith et al. 1998). Interestingly, none of the compact OH sources is coincident with any compact radio continuum source, implying a lower limit of the amplification factor of $\sim$100.

Each of the compact OH sources displays emission with a velocity range of 30–100 km s^{-1}. The brightness temperature of the compact OH maser emission is high, $T_b \sim 10^{10}$ K. And, the 1665 MHz line is conspicuously absent in the compact sources, with the 1667/1665 line ratio exceeding 100. One-third of the total flux density is undetected and must be in a diffuse component. The diffuse emission contains both the 1667 MHz and 1665 MHz line and the line ratio is near 1.8, the ratio of the line strengths (Rovilos et al. 2003). However, all the OH mega-maser emissions, including the diffuse component, are contained within the OH features determined by MERLIN (Figure 8; P. Diamond and E. Rovilos, private communication).

9.2. III Zw 35

III Zw 35 is a pair of interacting galaxies separated by 9″ (4.7 kpc) at PA $\approx 20°$. The OH emission and the radio continuum, $\leq$160 pc in extent, are found only in the northern galaxy nucleus which emits most of the total 10–120 μm luminosity of $3.5 \times 10^{11}\ L_{\odot}$ (Chapman et al. 1990). The OH emission source itself is elongated roughly N–S (PA $\approx -20°$) with a size $\leq$100 pc and a velocity gradient, suggesting a rotating disk of about 80 mas (40 pc) in extent (Montgomery & Cohen 1992).

When observed with VLBI, the 50 pc rotating disk is largely resolved out. In other words, emission with size scales larger than $1/2$ of the fringe spacing of the shortest baseline is not detected by the interferometer. As a result of this spatial filtering, only $\sim$60% of the OH mega-maser emission is detected in VLBI observations and found to be distributed in two clumps, each spread over $\sim$20 mas ($\sim$10 pc) and separated by 90 mas ($\sim$50 pc) essentially N–S (PA = $-20°$) (Figure 9) (Trotter et al. 1997, Diamond et al. 1999).

By combining data from MERLIN and the European VLBI Network (EVN), which provides spacings from tens to thousands of kilometers, Pihlström et al. (2001) recovered all the OH flux density and showed that the OH mega-masers come from two bright areas (containing the two bright clumps above) connected by fainter emission regions. The OH maser emission source can be modeled by pc-size OH maser clouds, with a small volume filling factor but a large velocity dispersion, within a nearly edge-on rotating torus (Figure 9). The compact OH mega-maser emission in this model arises from the tangent points of the edge-on torus where the gain path length is largest, with a significant chance of two or three clouds superimposed such that the foreground maser cloud amplifies the background one to produce strong maser emission (Deguchi 1981, Pihlström et al. 2001). Further refinement of this model suggests that the observed diffuse and compact OH mega-maser emission can be explained by a single phase of clumpy gas distributed in a thin ring structure and amplifying background continuum (Parra et al. 2004). While this model needs more physics to account for all the observations of III Zw 35 and other OH mega-maser sources, this study provides an attractive model to account for simultaneously the compact and diffuse emissions from OH mega-masers.

9.3. Arp 299

Arp 299 consists of two interacting galaxies, IC 694 and NGC 3690, but there are many sites of active star formation (Gallais et al. 2004; Gehrz, Sramek & Weedman 1983). However, the OH mega-maser emission is found only in the nucleus of IC694 (Baan & Haschick 1990), a massive galaxy nucleus undergoing an extended-duration starburst and accounting for $3 \times 10^{11}\ L_{\odot}$, about 50% of the total luminosity of the system. MERLIN observations resolved the OH mega-maser into a 100 pc rotating structure with a velocity gradient of 2.75 km $s^{-1}pc^{-1}$, oriented at PA $= 135°$ (Polatidis & Aalto 2000, 2001). CO emission is found in all the sites of active star formation, but the most intense and compact ($\leq$250 pc)

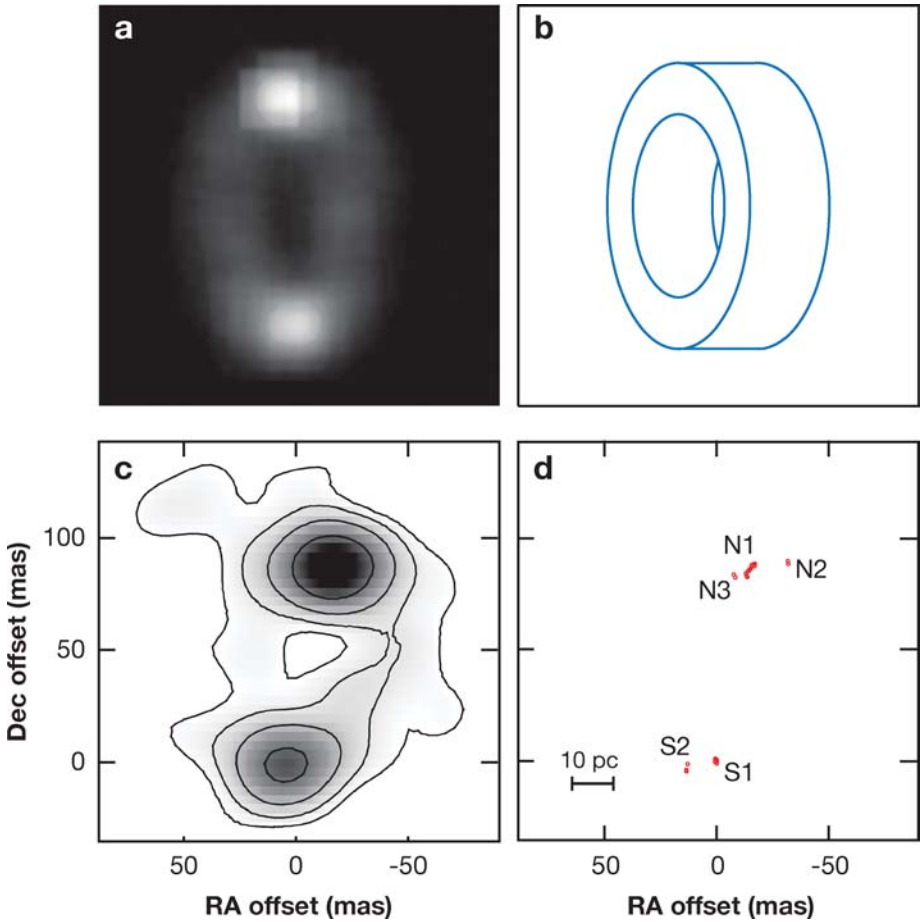

Figure 9 III Zw 35: The *top two panels* show the model of OH mega-maser emission with the simulated OH maser-emission source on the *left*; and the *bottom two panels* show the observed distribution of OH mega-maser emission, from the combined MERLIN+EVN observations (Pihlström et al. 2001) on the *left* and VLBI only (Diamond et al. 1999) on the right.

emission comes from $4 \times 10^9 M_\odot$ of molecular gas in the nucleus of IC 694, which is similar to the distribution of the radio continuum emission (Sargent & Scoville 1991; Aalto, Radford & Scoville 1997). The nuclear region of IC 694 harbors enshrouded massive star formation activity, even though it is not the youngest (Gallais et al. 2004). While all the sites of activity in Arp 299 contain the presumed conditions for OH mega-maser emission (such as the presence of radio continuum emission, molecular gas bathed in IR radiation powered by the young stars, and

large velocity dispersion), only the nucleus of IC 694, with the most molecular gas and the highest density as it is the only location with strong HCN emission (Aalto, Radford & Scoville 1997), is an OH mega-maser source. Do the other sites not exhibit OH mega-maser emission because that phase is over or has not begun, or because the physical conditions are simply not appropriate? Further studies of the properties of the different star forming sites in Arp 299 are clearly indicated.

9.4. Summary of High-Resolution Observations

It appears that OH mega-maser sources are typically of the order of 100 pc in extent. Except for Mrk 231 (Lonsdale et al. 2003), a fraction ($\sim$30%) of the OH mega-maser emission is diffuse, spread over the 100-pc scale structure, while the balance of the emission is found in compact structures of tens of pc in size. However, the compact sources are not coincident with peaks of compact radio continuum emission, and appear to emit primarily in the 1667 MHz line. The emission from the compact sources has a substantial linewidth of tens of km s^{-1}. The diffuse component appears to have both 1667 MHz and 1665 MHz emissions with the optically thin LTE line ratio, but also with a large linewidth.

Because ground-based VLBI observations at λ18 cm have maximum resolution of a few pc at the typical distance of the OH mega-masers, internal structures in the compact OH mega-maser sources may be unresolved. Given the velocity coherence needed for stimulated emission, the broad linewidth within the 10-pc scale compact structures (several tens of km s^{-1}) implies each compact source consists of a collection of unresolved maser sources (spots) with narrow linewidths. Also, the measured brightness temperature ($T_b \sim 10^{10}$ K) of the compact OH mega-maser emission, though high, is much less than 10^{12} K, the brightness temperature of Galactic OH maser spots (spatially resolved at the 10^{13}-cm scale). This suggests that the maser spots in the compact sources have a total areal filling factor of $\sim 10^{-2}$, which is much larger than what is seen in Galactic maser sources ($\sim 10^{-8}$). This result and the very large 1667/1665 line ratio in the compact OH sources may be explainable in the model presented for III Zw 35 in which the bright compact sources are due to the superposition and amplication of two or more maser clouds or clumps, which might be identified with the unresolved maser spots mentioned above (Parra et al. 2004). The 1667 MHz line is preferentially amplified by the superposed clouds if the OH clouds have higher gain in that line, leading to a large final 1667/1665 line ratio.

10. SOURCE OF OH MEGA-MASER EMISSION

10.1. Excitation Conditions of OH Mega-Masers

The characteristics of the λ18 cm OH mega-maser emission differ from those of Galactic maser sources, such as the main line intensity ratio ($T_{1667\,\mathrm{MHz}}$/

$T_{1665\ \mathrm{MHz}} > 1$), large linewidth ($>100$ km s^{-1}), and unpolarized emission.[13] Both the $\lambda 6$ cm ($^2\Pi_{3/2}\, J = 5/2$) and $\lambda 5$ cm ($^2\Pi_{1/2}\, J = 1/2$) OH lines, from the rotationally excited levels 120 K and 182 K above the ground state, respectively (Figure 1), have been detected in absorption from Arp 220, again in contrast to Galactic sources where they are typically in emission (Henkel, Guesten & Batrla 1986; Henkel, Guesten & Baan 1987). By comparing the velocity range of the emission and absorption, different regions of the source can be identified, and for the region where OH mega-maser emission originates, comparison of the excitation of the transitions from the ground and excited OH levels can be used to discriminate among the various schemes of pumping the OH mega-maser emission. Such analyses suggest that the observations can be explained by a radiative pump based on an intense FIR and nonthermal microwave photons in a region with $T_{\mathrm{dust}} \approx T_{\mathrm{rot}} \sim 60$ K (Henkel, Guesten & Baan 1987).

Detailed analysis of the effect of gas and dust temperatures, OH density, total gas density, velocity fields, and microturbulence on OH mega-maser emission has been carried out (Randell et al. 1995). Low-density ($10^{3.5}$–$10^{4.5}$ cm^{-3}) compact clouds ($\sim$3 pc), with warm dust ($T_{\mathrm{d}} > T_{\mathrm{k}} > 40$ K–50 K) and OH density of $\sim 10^4$ cm^{-3}, are radiatively pumped to yield dominant 1667 MHz emission for a wide range of conditions when amplifying compact nuclear radio cores. As such, conditions are not extraordinary; the factors that distinguish the LIRGs with OH mega-maser emission from the LIRGs without still need to be identified.

The $\lambda 6.2$ cm 1_{10}–1_{11} formaldehyde (H_2CO) transition, which is normally seen in absorption in the Galaxy, has also been detected in emission toward Arp 220 (Baan, Guesten & Haschick 1986), which has been confirmed recently, along with the emission from two other OH mega-masers (Araya, Baan & Hofner 2004). To account for the $\lambda 6.2$ cm 1_{10}–1_{11} formaldehyde maser emission, it was proposed that the inversion can be provided by microwave radiation (Boland & de Jong 1981). If the 6.2 cm formaldehyde maser emission originates from the same region as the OH mega-maser emission, the physical conditions would be appropriate for inverting the populations of the appropriate levels in both molecules. One common ingredient appears to be the role of microwave radiation in the pumping process.

Weak extended anomalous OH emission ($\geq$1 pc) has been seen in warm IR star-forming regions in the Galaxy, with very similar OH emission characteristics as extragalactic OH mega-maser emission: the 1667 MHz line stronger than the 1665 MHz line, linewidth of 3–5 km s^{-1}, and both unpolarized. It was suggested that OH mega-maser emission is due to a collection of these clouds: 10^6 such clouds totaling $10^9\ M_\odot$ of molecular gas (Mirabel, Rodriguez & Ruiz 1989). Further studies of the physical conditions responsible for these anomalous OH emission clouds in

[13] Methanol (CH_3OH) emission is often found alongside Galactic OH Type I masers associated with compact HII regions (Menten 1991). Surveys of methanol transition from OH mega-masers have set stringent limits on the methanol line, providing another indicator that the OH mega-maser emission is fundamentally different from the Galactic OH masers in star formation regions (Darling et al. 2003, Ellingsen et al. 1994, Phillips et al. 1998).

the Galaxy would help to understand the conditions leading to OH mega-maser emission.

10.2. OH Mega-Maser Sources and Extreme Starburst Regions

High-resolution observations of a few OH mega-maser sources show that the typical OH mega-maser source has an extent $\leq$100 pc and is found in a high concentration of molecular gas ($M_{H_2} \sim 10^9\ M_\odot$) in which intense starbursts ($L_{FIR} \sim 2 \times 10^{11}\ L_\odot$ with $\sim 10^9\ M_\odot$ in young stars) are taking place. This "extreme starburst region" could be in a rotating disk or torus, with physical conditions far more extreme than those found in molecular clouds in the disks of galaxies. Unlike the Galactic disk where the volume filling factor, f_V, of self-gravitating giant molecular clouds of 300 cm^{-3} mean density is only a few percent, $f_V \sim 1$ in these extreme starburst regions which have an average density of $n(H_2) \leq 10^4$ cm^{-3} and a radiation field of $\sim 10^5$ G_o,[14] a velocity dispersion of $\sigma_V \approx 100$ km s^{-1}, and a gas and dust temperature of $\sim$65–100 K. Given the correlation of radio continuum and IR radiation from galaxies and star formation regions (Condon 1992), the radio radiation field would be correspondingly strong along with the IR radiation field in these extreme starburst regions. As high-density tracers such as CS and HCN are also detected, $\sim$10% of the gas has to be in self-gravitating clouds of gas density $\sim 10^5$ cm^{-3}. Compared to Galactic giant molecular clouds, these regions are five times larger, 3000 times more massive, and 10^5 times more IR luminous due to the embedded OB stars (Downes & Solomon 1998). The abundance and high space density of young stars in the extreme starburst regions would also be very favorable for photoevaporation of water condensed on grains (which becomes effective at a dust temperature $T_d > 100$ K) and photodissociation of the water to produce OH, leading to an elevated OH abundance.

Thus, it is very suggestive that conditions in the extreme starburst regions are appropriate for producing OH mega-maser emission. In particular, the extreme starburst regions possess much stronger FIR and microwave radiation fields compared to the environments of Galactic OH Type I masers. They would provide the physical setting in which the model of OH mega-maser emission of Parra et al. (2004) can operate. Whether or not all OH mega-maser sources can be identified with such extreme starburst regions will have to be confirmed observationally. Also needed is more detailed analysis of the OH excitation under the conditions prevailing in such regions to confirm that OH mega-maser emission can be explained by this model.

The spatial coincidence of the OH mega-maser emission and radio continuum on the 100-pc scale may simply indicate that both originate from the extreme starburst

[14] G_o is the ratio of the UV radiation field to the "normal" Galactic interstellar UV radiation field.

region and that the maser emission is not necessarily a result of amplification of the background continuum emission. Some OH mega-maser line profiles display extended blueshifted wings which can be explained as molecular outflows from starburst-driven superwinds (Baan & Haschick 1987; Baan, Haschick & Henkel 1989). This further suggests that the OH mega-maser emission is physically related to starburst regions, and therefore likely to be a short-lived phenomenon.

In this context, NGC 6240 poses an interesting case of a luminous IR galaxy that does not display OH mega-maser emission. NGC 6240 is a prototypical luminous IR galaxy with $L_{\rm FIR} \approx 6 \times 10^{11}\ L_{\odot}$ and contains two NIR nuclei $\sim$1.6″ (750 pc) apart. CO observations have shown that $\sim$1–2 $\times$ $10^9\ M_{\odot}$ of molecular gas exist in a rotating but highly turbulent thick disk (radius $\approx$250 pc centered between the two nuclei and a comparable amount of gas distributed more extensively (Tacconi et al. 1999)). The radio continuum has two peaks coinciding with the NIR nuclei and extensions but does not overlap with the CO emission. Given the $L_{\rm OH} \propto L_{\rm FIR}^{1.2}$ correlation, the presence of a large quantity of molecular gas and radio continuum sources, NGC 6240 would be a strong OH mega-maser, and yet it exhibits only OH absorption (Baan et al. 1985). It is suggestive that conditions for OH mega-maser emission are found only in regions where an ongoing intense starburst is physically embedded in the molecular gas, whereas the large molecular disk in NGC 6240 has not reached the conditions for initiating the starburst (Tacconi et al. 1999) or has already past the phase of extreme starbursts.

11. SUMMARY

Mega-masers are remarkable natural phenomena. As radio stations, they have the equivalent transmitting power of the order of ten trillion trillion megawatt and we can receive their signals possibly from as far as the edge of the Universe[15]. Maser emission occurs in nature because conditions in the interstellar medium are typically not in thermal equilibrium, and it is apparently not uncommon to find dense gas with the right conditions in the vicinity of stars or active galactic nuclei that maintain an inverted population in the maser molecules.

Water mega-masers, with isotropic luminosity up to $\sim 10^4\ L_{\odot}$, are found typically within the central parsec of an AGN, characterized as Seyfert2 or LINER, either in a circumnuclear accretion disk that is directly heated by the radiation from the AGN or in the surrounding molecular gas excited by the nuclear wind or jet, or both. The mass of the molecular gas involved in the mega-maser emission is modest, on the order of $10^5\ M_{\odot}$ or less. In contrast to Galactic water masers that derive their energy from stars, water mega-masers derive their energy from the AGN ultimately. Because of the high-surface brightness of maser emission, water

[15]It is interesting to speculate if such power transmitters can be harnessed by an advanced civilization for communication across the cosmos.

mega-masers can be observed at submilliarcsecond resolution providing subparsec resolution of the region immediately surrounding the AGN in galaxies out to 10 Mpc, a very powerful tool that has been used to delineate a possibly thin Keplerian accretion disk in NGC 4258 and to determine the mass distribution within the central 0.1 pc, providing a highly compelling case for a massive black hole at the galactic nucleus.

The number of known water mega-masers is relatively small (around 65 currently, out of more than 1000 searched). Why are they so rare? High-resolution studies show that the water mega-maser emission is directional and the small emission solid angle would explain their low detection rate. In addition, their lifetime could be short, given the delicate balance of conditions of high-density gas that is being excited either directly by the intense radiation of the AGN or by an energetic jet or mass outflow, all of which are known to be variable.

Hydroxyl mega-masers, with luminosity up to $10^4\ L_\odot$ or more, are found only in LIRGs. There is a good correlation between the OH luminosity and the IR luminosity: $L_{\rm OH} \propto L_{\rm FIR}^{1.2}$, although 80% of the LIRGs surveyed do not show OH mega-maser emission. high-resolution observations have shown that the OH mega-maser emission is extended from 10-pc to 100-pc scale, and the 100-pc scale spatial extent of the emission region is primarily responsible for the large observed flux density of OH mega-masers. The clear correlation of OH mega-maser emission with intense IR radiation field is expected from the pumping mechanisms of OH maser emission. While the model of amplification of background radio continuum emission by foreground OH clouds has been widely discussed, the conditions for achieving population inversion over the much larger extent of OH mega-maser sources compared to the Galactic maser sources and the presumably special conditions in 20% of the LIRGs to produce OH mega-maser emission are not yet well understood.

Current observations indicate that OH mega-masers are found in extreme starburst regions in LIRGs, where the conditions apparently are conducive to the formation of a very large number of OH maser sources that collectively produce the mega-maser emission, but further elucidation of the physics involved is required. Are all the OH mega-masers coincident with extreme starburst regions? What are the physical conditions in these regions that produce OH mega-maser emission? Does this hypothesis imply that 80% of the LIRGs searched but showing no OH mega-maser emission have no extreme starburst regions?

To address these and other issues in understanding mega-masers, the Atacama Large Millimeter Array (ALMA) will be very powerful. For example, observing submm water maser lines will add additional constraints to the physics of water mega-masers. To study the extreme starburst regions that produce OH mega-maser emission, ALMA will have the requisite sensitivity, frequency coverage (31–950 GHz), and resolution ($\geq$5 mas) that are ideally suited to probe the physical conditions of the molecular medium in such regions.

Currently, H_2O and OH mega-masers are not known to exist in the same galaxy, which has raised the question whether they are mutually exclusive (Lonsdale 2002).

Given that H_2O mega-masers are found typically within the central parsec of an AGN and OH mega-masers are associated with starburst regions that are distributed over a 100-pc scale, the occurrence of the two types of masers in the same galaxy is not physically excluded. Their relationship is analogous to that between AGNs and starbursts. The two kinds of mega-masers are not known to overlap in the same galaxy so far presumably because first of all mega-masers are rare and second the samples searched tend not to overlap. For example, OH mega-maser candidates have been selected according to the high-IR luminosity out to $z < 0.3$, whereas the H_2O mega-masers searches have concentrated on nearby galaxies (predominantly spirals) with AGN characteristics at relatively low redshift ($z < 0.1$, so far).

With a suite of other powerful new facilities in the centimeter and longer wavelength range coming into operation in the coming decade, the observations of mega-masers will become increasingly important because many of the valuable applications will become more routine. Such new telescopes include the Green Bank Telescope (GBT), the Expanded VLA (EVLA), and eventually the Square Kilometre Array (SKA) with an effective area $A_e \sim 10^6$ m^2. They will enable the detection of mega-masers, and giga-masers, at redshift z of a few, and in more diverse environments. Because of the substantial increase of sensitivity, the SKA will increase the number of known OH and H_2O mega-maser sources by factors of between 10^2 and 10^3, leading to 10^5–10^6 sources (Morganti et al. 2004). Observing the mega-maser emission lines with the SKA enables the determination of the redshifts and thus the luminosities for some of the most distant and optically faint star-forming galaxies and active galactic nuclei, even those galaxies that are deeply enshrouded in dust or shining prior to the end of reionization (Blain et al. 2004). In contrast to optical and IR radiation that is typically thermal, maser emission by definition has extremely high-surface brightness which enables the very-high-resolution probes of active galaxies during the most active phase of star formation at $z \sim 2$, providing detailed information on the spatial structure, dynamics, and physical conditions of galactic nuclei and starburst regions, otherwise impossible to obtain.

ACKNOWLEDGMENTS

I have benefitted greatly from discussions and exchanges with many colleagues, including E. Bergin, J. Braatz, R. Cesaroni, J. Darling, P. Diamond, D. Downes, E. Falgarone, C. Gammie, L. Greenhill, C. Henkel, M.-C. Liang, F. Mirabel, J. Moran, R. Norris, Y. Pihlström, A. Tarchi, B. Turner, E. van Dishoeck, M. Walmsley, W. Watso, and M.S. Yun. I would like to thank R. Blandford for comments and interesting suggestions. The writing of this review started in earnest during a visit in the summer of 2002 to the Institute for Astronomy (IfA) of the University of Hawaii. I wish to thank R. Kudritzky and his colleagues at the IfA for their hospitality. Research at the Institute of Astronomy and Astrophysics is supported by the Academia Sinica in Taipei and in part by the National Science

Council of Taiwan. The National Radio Astronomy Observatory is supported by the National Science Foundation and operated by the Associated Universities, Inc.

The *Annual Review of Astronomy and Astrophysics* is online at http://astro.annualreviews.org

LITERATURE CITED

Aalto S, Radford SJE, Scoville NZ, Sargent AI. 1997. *Astrophys. J. Lett.* 475:L107

Andersen J. 1998. *Hi. Astron.*, pp. 11

Andrew BH, Bell MB, Broten NW, MacLeod JM. 1975. *Astron. Astrophys.* 39:421

Antonucci R. 1993. *Annu. Rev. Astron. Astrophys.* 31:473

Antonucci RRJ, Miller JS. 1985. *Astrophys. J.* 297:621

Araya E, Baan WA, Hofner P. 2004. *Astrophys. J. Suppl.* 154:541

Argon AL, Greenhill LJ, Moran JM, Reid MJ, Menten KM, et al. 1994. *Astrophys. J.* 422:586

Argon AL, Greenhill LJ, Moran JM, Reid MJ, Menten KM, Inoue M. 2004. *Astrophys. J.* 615:702

Argon AL, Reid MJ, Menten KM. 2003. *Astrophys. J.* 593:925

Baan WA. 1985. *Nature* 315:26

Baan WA. 1996. High-Sensitivity Radio Astronomy. *Proc. Jodrell Bank, Univ. Manch., Jan 22–26, 1996*. ed. D Jackson, pp. 73. Cambridge: Cambridge Univ. Press

Baan WA. 1989. *Astrophys. J.* 338:804

Baan WA. 1998. *Hi. Astron.* 11:937

Baan WA, Haschick AD. 1984. *Astrophys. J.* 279:541

Baan WA, Haschick AD. 1987. *Astrophys. J.* 318:139

Baan WA, Haschick AD. 1990. *Astrophys. J.* 364:65

Baan WA, Haschick AD. 1994. *Astrophys. J. Lett.* 424:L33

Baan WA, Haschick AD, Buckley D, Schmelz JT. 1985. *Astrophys. J.* 293:394

Baan WA, Haschick AD, Henkel C. 1989. *Astrophys. J.* 346:680

Baan WA, Guesten R, Haschick AD. 1986. *Astrophys. J.* 305:830

Baan WA, Klockner H. 2001. ASP Conf-Ser249: *The Central Kiloparsec of Starbursts and AGN: The La Palma Connection*. 639

Baan WA, Rhoads J, Fisher K, Altschuler DR, Haschick AD. 1982. *Astrophys. J. Lett.* 396:L99

Baan WA, Rhoads J, Fisher K, Altschuler DR, Haschick AD. 1992. *Astrophys. J. Lett.* 396:L99

Baan WA, Schmelz JT, Haschick AD. 1985. *Astrophys. J. Lett.* 298:L51

Baan WA, Wood PA, Haschick AD. 1982. *Astrophys. J. Lett.* 260:L52

Barvainis R, Antonucci R. 2005. *Astrophys. J. Lett.* In press

Batchelor RA, Jauncey DL, Whiteoak JB. 1982. *Mon. Not. R. Astron. Soc.* 200:19P

Baudry A, Brouillet N. 1996. *Astron. Astrophys.* 316:188

Becker R, Henkel C, Wilson TL, Wouterloot JGA. 1993. *Astron. Astrophys.* 268:483

Bergin EA, Melnick GJ, Stauffer JR, Ashby MLN, Chin G, et al. 2000. *Astrophys. J. Lett.* 539:L129

Blain AW, Carilli C, Darling J. 2004. *New Astron. Rev.* 48:1247

Blain AW, Smail I, Ivison RJ, Kneib J-P, Frayer DT. 2002. *Ph. Rev. Phys.* 369:111

Boland W, de Jong T. 1981. *Astron. Astrophys.* 98:149–54

Bottinelli L, Fraix-Burnet D, Gouguenheim L, Kazes I, Le Squeren AM, et al. 1985. *Astron. Astrophys.* 151:L7

Braatz JA. 2002. *IAU Symp.* 206:396

Braatz JA, Henkel C, Greenhill LJ, Moran

JM, Wilson AS. 2004. *Astrophys. J. Lett.* 617:L29–32

Braatz JA, Wilson AS, Henkel C. 1996a. *Astrophys. J.* 106:51

Braatz JA, Wilson AS, Henkel C. 1996b. *V. Astron.* 40:83

Braatz JA, Wilson AS, Henkel C. 1997. *Astrophys. J.* 110:321

Braatz JA, Wilson AS, Henkel C, Gough R, Sinclair M. 2003. *Astrophys. J.* 146:249

Bragg AE, Greenhill LJ, Moran JM, Henkel C. 2000. *Astrophys. J.* 535:73

Briggs FH. 1998. *Astron. Astrophys.* 336: 815

Brunthaler A, Reid M, Falcke H, Greenhill LJ, Henkel C. 2002. *Proc. 6th EVN Symp.*, pp. 189

Bryant PM, Scoville NZ. 1996. *Astrophys. J.* 457:678

Burdiuzha VV, Komberg BV. 1990. *Astron. Astrophys.* 234:40

Carilli CL, Yun MS. 1999. *Astrophys. J. Lett.* 513:L13

Carilli CL, Yun MS. 2000. *Astrophys. J.* 530:618

Cernicharo J, Thum C, Hein H, John D, Garcia P, Mattioco F. 1990. *Astron. Astrophys.* 231:L15

Cesaroni R, Walmsley CM. 1991. *Astron. Astrophys.* 241:537

Chandra DA, Varshalovich DA, Kegel WH. 1984. *Astron. Astrophys. Suppl.* 55:51

Chapman JM, Staveley-Smith L, Axon DJ, Unger SW, Cohen RJ, et al. 1990. *Mon. Not. R. Astron. Soc.* 244:281

Cheung AC, Rank DM, Townes CH, Thornton DD, Welch WJ. 1969. *Nature* 221:626

Churchwell E, Witzel A, Huchtmeier W, Pauliny-toth I, Roland J, Wieber W. 1977. *Astron. Astrophys.* 54:969

Clark BG, Kellermann KI, Bare CC, Cohen MH, Jauncey DL. 1968. *Astrophys. J. Lett.* 153:L67

Claussen MJ, Diamond PJ, Braatz JA, Wilson AS, Henkel C. 1998. *Astrophys. J. Lett.* 500:L129

Claussen MJ, Heiligman GM, Lo KY. 1984. *Nature* 310:298

Claussen MJ, Lo KY. 1986. *Astrophys. J.* 308:592

Claussen MJ, Reid MJ, Schneps MH, Lo K-Y, Moran JM, Güsten R. 1988. *IAU Symp. 129: The Impact of VLBI on Astrophysics and Geophysics*. 129:231

Clegg AW, Nedoluha GE. 1993. Lecture Notes in Physics. Vol. 412. *Proc. Conf. Astrophys. Masers, Arlington, VA, Mar. 9–11, 1992*. Berlin: Springer-Verlag

Cohen RJ. 1998. *Hi. Astron.* 11:938

Collison AJ, Watson WD. 1995. *Astrophys. J. Lett.* 452:L103

Condon JJ. 1992. *Annu. Rev. Astron. Astrophys.* 30:575

Darling J. 2003. *The astrochemistry of external galaxies. 25th Meeting of the IAU, Joint Discussion 21*, Sydney, Australia, 23 July 2003, p. 21

Darling J, Giovanelli R. 2000. *Astron. J.* 119: 3003

Darling J, Giovanelli R. 2001. *Astron. J.* 121: 1278

Darling J, Giovanelli R. 2002a. *Astron. J.* 124: 100

Darling J, Giovanelli R. 2002b. *Astrophys. J. Lett.* 569:L87

Darling J, Giovanelli R. 2002c. *Astrophys. J.* 572:810

Darling J, Goldsmith P, Li D, Giovanelli R. 2003. *Astron. J.* 125:1177

de Jong T. 1973. *Astron. Astrophys.* 26:297

Deguchi S. 1981. *Astrophys. J.* 249:145

Deguchi S. 1994. *Astrophys. J.* 420:551–57

Deguchi S, Watson WD. 1989. *Astrophys. J. Lett.* 340:L17

Desch SJ, Wallin BK, Watson WD. 1998. *Astrophys. J.* 496:775

Diamond PJ, Lonsdale CJ, Smith HE. 1999. *Astrophys. J.* 511:178

Dickey JM, Planesas P, Mirabel IF, Kazes I. 1990. *Astron. J.* 100:1457

Dickinson DF, Chaisson EJ. 1971. *Astrophys. J.* 169:207

Dos Santos PM, Lepine JRD. 1979. *Nature* 278:34

Downes D, Solomon PM. 1998. *Astrophys. J.* 507:615

Draine BT, Roberge WG, Dalgarno A. 1983. *Astrophys. J.* 264:485
Draine BT, Woods DT. 1991. *Astrophys. J.* 383:621
Dulk GA. 1985. *Annu. Rev. Astron. Astrophys.* 23:169
Eckart A, Ott T, Genzel R. 1999. *Astron. Astrophys.* 352:L22
Elitzur M. 1992a. *Annu. Rev. Astron. Astrophys.* 30:75
Elitzur M. 1992b. *Astronomical Masers*. Dordrecht: Kluwer
Elitzur M, Hollenbach DJ, McKee CF. 1989. *Astrophys. J.* 346:983
Ellingsen SP, Norris RP, Whiteoak JB, Vaile RA, McCullch PM, Price MG. 1994. *Mon. Not. R. Astron. Soc.* 267:510
Elmegreen BG, Morris M. 1979. *Astrophys. J.* 229:593
Falcke H, Henkel C, Peck AB, Hagiwara Y, Prieto MA, Gallimore JF. 2000. *Astron. Astrophys.* 358:L17
Gallais P, Charmandaris V, Le Floc'h E, Mirabel IF, Sauvage M, et al. 2004. *Astron. Astrophys.* 414:845
Gallimore JF, Baum SA, O'Dea CP, Brinks E, Pedlar A. 1996. *Astrophys. J.* 462: 740
Gallimore JF, Henkel C, Baum SA, Glass IS, Claussen MJ, et al. 2001. *Astrophys. J.* 556:694
Gammie CF, Narayan R, Blandford R. 1999. *Astrophys. J.* 516:177
Gardner FF, Whiteoak JB. 1975. *Mon. Not. R. Astron. Soc.* 173:77P
Gardner FF, Whiteoak JB. 1982. *Mon. Not. R. Astron. Soc.* 201:13P
Gehrz RD, Sramek RA, Weedman DW. 1983. *Astrophys. J.* 267:551
Genzel R, Downes D. 1977. *Annu. Rev. Astron. Astrophys.* 30:145
Genzel R, Downes D, Moran J, Johston KJ, Spencer J, et al. 1978. *Astron. Astrophys.* 66:13
Ghez AM, Klein BL, Morris M, Becklin EE. 1998. *Astrophys. J.* 509:678
Goldreich P, Kwan J. 1974. *Astrophys. J.* 191:93
Gordon JP, Zeiger HJ, Townes CH. 1955. *Phys. Rev.* 95:282L
Graham JR, Carico DP, Matthews K, Neugebauer G, Soifer BT, Wilson TD. 1990. *Astrophys. J. Lett.* 354:L5
Greenhill LJ. 1997. ASP Conf Ser 113: IAU Colloq 159: *Emission Lines in Active Galaxies: New Methods and Techniques*, pp. 394
Greenhill LJ. 2002. *IAU Symposium* 206: 381
Greenhill LJ, Ellingsen SP, Norris RP, Mc Gregor PJ, Gough RG, et al. 2002. *Astrophys. J.* 565:836
Greenhill LJ, Ellingsen SP, Norris RP, Gough RG, Sinclair MW, et al. 1997. *Astrophys. J. Lett.* 474:L103
Greenhill LJ, Gwinn CR. 1997. *Astrophys. Space Sci.* 248:261
Greenhill LJ, Gwinn CR, Antonucci R, Barvainis R. 1996. *Astrophys. J. Lett.* 472:L21
Greenhill LJ, Henkel C, Becker R, Wilson TL, Wouterloot JGA. 1995a. *Astron. Astrophys.* 304:21
Greenhill LJ, Jiang DR, Moran JM, Reid MJ, Lo KY, Claussen MJ. 1995b. *Astrophys. J.* 440:619
Greenhill LJ, Moran JM, Reid MJ, Gwinn CR, Menten KM, et al. 1990. *Astrophys. J.* 364:513
Greenhill LJ, Kondratko PT, Lovell JEJ, Kuiper TBH, Moran JM, et al. 2003a. *Astrophys. J. Lett.* 582:L11
Greenhill LJ, Booth RS, Ellingsen SP, Herrnstein JR, Jauncy DL, et al. 2003b. *Astrophys. J.* 590:162
Gundermann E. 1965. PhD Thesis. Harvard Univ. Cambridge, Mass.
Hagiwara Y, Diamond PJ, Miyoshi M. 2002. *Astron. Astrophys.* 383:65
Hagiwara Y, Diamond PJ, Miyoshi M. 2003. *Astron. Astrophys.* 400:457
Hagiwara Y, Henkel C, Menten KM, Nakai N. 2001. *Astrophys. J. Lett.* 560:L37
Hagiwara Y, Henkel C, Sherwood WA, Baan WA. 2002. *Astron. Astrophys.* 387:L29
Hartquist TW, Menten KM, Lepp S, Dalgarno A. 1995. *Mon. Not. R. Astron. Soc.* 272:184
Haschick AD, Baan WA. 1985. *Nature.* 314:144

Haschick AD, Baan WA. 1990. *Astrophys. J. Lett.* 355:L23

Haschick AD, Baan WA, Peng EW. 1994. *Astrophys. J. Lett.* 437:L35

Haschick AD, Baan WA, Schneps MH, Reid MJ, Moran JM, Guesten R. 1990. *Astrophys. J.* 356:149

Henkel C, Braatz JA. 2003. *Acta Astronomica Sinica* 44:55

Henkel C, Braatz JA, Greenhill LJ, Wilson AS. 2002. *Astron. Astrophys.* 394:L23

Henkel C, Guesten R, Baan WA. 1987. *Astron. Astrophys.* 185:14

Henkel C, Guesten R, Batrla W. 1986. *Astron. Astrophys.* 168:L13

Henkel C, Guesten R, Downes D, Thum C, Wilson TL, Biermann P. 1984. *Astron. Astrophys.* 141:L1

Henkel C, Tarchi A, Menten KM, Peck AB. 2004. *Astron. Astrophys.* 414:117

Henkel C, Wang YP, Falcke H, Wilson AS, Braatz JA. 1998. *Astron. Astrophys.* 335:463

Henkel C, Wilson TL. 1990. *Astron. Astrophys.* 229:431

Henkel C, Wouterloot JGA, Bally J. 1986. *Astron. Astrophys.* 155:193

Herrnstein JR, Moran JM, Greenhill LJ, Diamond PJ, Inoue M, et al. 1999. *Nature* 400:539

Herrnstein JR, Greenhill LJ, Moran JM, Diamond PJ, Inoue M, et al. 1998a. *Astrophys. J. Lett.* 497:L69

Herrnstein JR, Moran JM, Greenhill LJ, Blackman EG, Diamond PJ. 1998b. *Astrophys. J.* 508:243

Ho PTP, Martin RN, Henkel C, Turner JL. 1987. *Astrophys. J.* 320:663

Hodge PW. 1981. *Annu. Rev. Astron. Astrophys.* 19:357

Hollenbach DJ, Tielens AGGM. 1997. *Annu. Rev. Astron. Astrophys.* 35:179

Huchtmeier WK, Eckart A, Zensus AJ. 1988. *Astron. Astrophys.* 200:26

Huchtmeier WK, Witzel A, Kuehr H, Pauliny-Toth II, Roland J. 1978. *Astron. Astrophys.* 64:L21

Hure JM. 2002. *Astron. Astrophys.* 395:L21

Ishihara Y, Nakai N, Iyomoto N, Makishima K, Diamond P, Hall P. 2001. *Publ. Astron. Soc. Japan* 53:215

Kameno S, Inoue M, Wajima K, Sawada-Satoh S, Shen Z. 2003. *Publ. Astron. Soc. Australia* 20:134

Kartje JF, Königl A, Elitzur M. 1999. *Astrophys. J.* 513:180

Klöckner HR, Baan WA. 2002. *IAU Symposium* 206:430

Klöckner HR, Baan WA, Garrett MA. 2003. *Nature* 421:821

Koda J, Sofue Y, Kohno K, Nakanishi H, Onodera S, et al. 2002. *Astrophys. J.* 573:105

Koekemoer AM, Henkel C, Greenhill LJ, Dey A, van Breugel W, et al. 1995. *Nature* 378:697

Kondratko PT, Greenhill LJ, Moran JM. 2005. *Astrophys. J.* 618:618

Königl A, Kartje JF. 1994. *Astrophys. J.* 434:446

Kormendy J, Richstone D. 1995. *Annu. Rev. Astron. Astrophys.* 33:581

Krolik JH, Kallman TR. 1983. *Astrophys. J.* 267:610

Krolik JH, Lepp S. 1989. *Astrophys. J.* 347:179

Kylafis ND. 1988. *IAU Symp 129: The Impact of VLBI on Astrophysics and Geophysics*. 129:223

Kylafis ND, Norman CA. 1990. *Astrophys. J.* 350:209

Kylafis ND, Norman CA. 1991. *Astrophys. J.* 373:525

Lasota J-P, Abramowicz MA, Chen X, Krolik J, Narayan R, Yi I. 1996. *Astrophys. J.* 462: 142

Lepp S, McCray R. 1983. *Astrophys. J.* 269:560

Lepp S, McCray R, Shull JM, Woods DT, Kallman T. 1985. *Astrophys. J.* 288:58

Litvak MM. 1974. *Annu. Rev. Astron. Astrophys.* 12:97

Lo K-Y. 1974. *Interstellar microwave radiation and early stellar evolution.* PhD Thesis. MIT

Lonsdale CJ. 2002. *IAU Symp*. 206:413

Lonsdale CJ, Diamond PJ, Smith HE. 1994. *Nature* 370:117

Lonsdale CL, Lonsdale CJ, Diamond PJ, Smith HE. 1998. *Astrophys. J. Lett.* 494:L239

Lonsdale CJ, Lonsdale CJ, Smith HE, Diamond PJ. 2003. *Astrophys. J.* 592:804
Lynden-Bell D. 1969. *Nature* 223:690
MacLow M, Elitzur M, Stone JM, Königl A. 1994. *Astrophys. J.* 427:914
Mader GL, Johnston KJ, Moran JM. 1978. *Astrophys. J.* 224:115
Madore BF, Freedman W, Silbermann N, Harding P, Huchra J, et al. 1999. *Astrophys. J.* 515:29
Maloney PR. 2002a. *Publ. Astron. Soc. Australia* 19:401
Maloney PR, Begelman MC, Nowak MA. 1998. *Astrophys. J.* 504:77
Maloney PR, Hollenbach DJ, Tielens AGGM. 1996. *Astrophys. J.* 466:561
Maoz E. 1995. *Astrophys. J. Lett.* 447:L91
Maoz E, McKee CF. 1998. ASP ConfSer144: IAU Colloq164: *Radio Emission from Galactic and Extragalactic Compact Sources*, pp. 217
Martin JM, Bottinelli L, Dennefeld M, Gougenheim L, Handa T, et al. 1988. *Astron. Astrophys.* 195:71
Martin JM, Bottinelli L, Gouguenheim L, Dennefeld M. 1991. *Astron. Astrophys.* 245: 393
Martin JM, Le Squeren AM, Bottinelli L, Gouguenheim L, Dennefeld M. 1989. *Astron. Astrophys.* 208:39
Menten KM. 1991. *Astrophys. J. Lett.* 380:L75
Menten KM, Melnick GJ, Phillips TG. 1990. *Astrophys. J. Lett.* 350:L41
Menten KM, Melnick GJ, Phillips TG, Neufeld DA. 1990. *Astrophys. J. Lett.* 363:L27
Menten KM, Young K. 1995. *Astrophys. J. Lett.* 450:L67
Migenes V, Reid MJ, eds. 2002. *Proc. IAU Symp. 206: Cosmic Masers: From Proto-Stars to Black Holes*
Millar TJ. 1996. *IAU Symp 178: Molecules in Astrophysics: Probes & Processes* 178:75
Mirabel IF, Rodriguez LF, Ruiz A. 1989. *Astrophys. J.* 346:180
Mirabel IF, Sanders DB. 1987. *Astrophys. J. Lett.* 322:688
Miyoshi M, Moran JM, Herrnstein J, Greenhill L, Nakai N, et al. 1995. *Nature* 373:127
Modjaz M, Moran JM, Greenhill LJ, Kondratko PT. 2003. *Quasar Cores and Jets*, 25th Meeting of the IAU, Joint Discussion 18, 23–24 July 2003, Sydney, Australia, 18
Montgomery AS, Cohen RJ. 1992. *Mon. Not. R. Astron. Soc.* 254:23P–26P
Moran J. 1984. *Nature* 310:270
Moran JM. 2000. *Phil. Trans. R. Soc. Lond.* A 358:797
Moran JM, Greenhill LJ, Herrnstein J, Diamond P, Miyoshi M, et al. 1995. *Proc. Natl. Acad. Sci. USA* 92:11427
Moran JM, Burke BF, Barrett AH, Rogers AEER, Carter JC, et al. 1968. *Astrophys. J. Lett.* 152:L97
Moran JM, Greenhill LJ. 1999. *J. Astrophys. Astron.* 20:165
Morganti R, Greenhill LJ, Peck AB, Jones DL, Henkel C. 2004. *New Astron. Rev.* 48:1195
Morris M, Serabyn E. 1996. *Annu. Rev. Astron. Astrophys.* 34:645
Mumma MJ, Buhl D, Chin G, Deming D, Espenak F, et al. 1981. *Science* 212:45
Mundell CG, Ferruit P, Pedlar A. 2001. *Astrophys. J.* 560:168
Nakai N, Takashi K. 1988. *Publ. Astron. Soc. Jpn.* 40:139
Nakai N, Inoue M, Miyazawa K, Miyoshi M, Hall P. 1995. *Publ. Astron. Soc. Japan* 47:771
Nakai N, Inoue M, Miyoshi M. 1993. *Nature* 361:45
Nakai N, Sato N, Yamauchi A. 2002. *Astrophys. J. Lett.* 54:L27
Neufeld DA. 2000. *Astrophys. J. Lett.* 542:L99
Neufeld DA, Maloney PR. 1995. *Astrophys. J. Lett.* 447:L17
Neufeld DA, Maloney PR, Conger S. 1994. *Astrophys. J. Lett.* 436:L127
Neufeld DA, Melnick GJ. 1991. *Astrophys. J.* 368:215
Norris RP. 1985. *Mon. Not. R. Astron. Soc.* 216:701
Norris RP, Gardner FF, Whiteoak JB, Allen DA, Roche PF. 1989. *Mon. Not. R. Astron. Soc.* 237:673
Palagi F, Cesaroni R, Comoretto G, Felli M, Natale V. 1993. *Astron. Astrophys. Sup.* 101:153

Papaloizou JCB, Terquem C, Lin DNC. 1998. *Astrophys. J.* 497:212
Parra R, Conway J, Elitzur M. 2005. *Astrophys. Space Sci.* 295:325–30
Peck AB, Henkel C, Ulvestad JS, Brunthaler A, Falcke H, et al. 2003. *Astrophys. J.* 590: 149
Phillips CJ, Ellingsen SP, Rayner DP, Norris RP. 1998. *Mon. Not. R. Astron. Soc.* 294: 265
Pihlström YM, Conway JE, Booth RS, Diamond PJ, Polatidis AG. 2001. *Astron. Astrophys.* 377:413
Polatidis AG, Aalto S. 2000. *EVN Symposium 2000, Proc. 5th European VLBI Network Symposium held at Chalmers University of Technology, Gothenburg, Sweden, June 29–July 1, 2000*, ed. JE Conway, AG Polatidis, RS Booth, YM Pihlström, Onsala Space Observatory, 127:127
Polatidis, AG, Aalto S. 2001. *IAU Symposium* 205:198
Pringle JE. 1996. *Mon. Not. R. Astron. Soc.* 281:357
Randell J, Field D, Jones, KN, Yates JA, Gray MD. 1995. *Astron. Astrophys.* 300:659
Rank DM, Townes CH, Welch WJ. 1971. *Science* 174:1083
Reid MJ. 2002. *IAU Symp.* 206:506
Reid MJ, Moran JM. 1981. *Annu. Rev. Astron. Astrophys.* 19:231
Rieu N-Q, Mebold U, Winnberg A, Guibert J, Booth R. 1976. *Astron. Astrophys.* 52:467
Rovilos E, Diamond PJ, Lonsdale CJ, Lonsdale CJ, Smith HE. 2003. *Mon. Not. R. Astron. Soc.* 342:373
Rowan-Robinson M. 2000. *Mon. Not. R. Astron. Soc.* 316:885
Ruiz M, Efstathiou A, Alexander DM, Hough J. 2001. *Mon. Not. R. Astron. Soc.* 325: 995
Sakamoto K, Scoville NZ, Yun MS, Crosas M, Genzel R, Tacconi LJ. 1999. *Astrophys. J.* 514:68
Salpeter EE. 1964. *Astrophys. J.* 140:796
Sargent A, Scoville N. 1991. *Astrophys. J. Lett.* 366:L1
Saunders W, Sutherland WJ, Maddox SJ, Keeble O, Oliver SJ, et al. 2000. *Mon. Not. R. Astron. Soc.* 317:55
Sawada-Satoh S, Inoue M, Shibata KM, Kameno S, Migenes V, et al. 2000. *Publ. Astron. Soc. Japan* 52:421
Sawada-Satoh S, Kameno S, Shibata KM, Inoue M. 2005. *Proc. Future Directions in High Resolution Astronomy: A Celebration of the 10th Anniversary of the VLBA, Socorro, New Mexico, USA.* In press
Scalise E, Braz MA. 1981. *Nature* 290:36
Scalise E, Braz MA. 1982. *Astron. J.* 87:528
Schinnerer E, Eckart A, Tacconi LJ, Genzel R, Downes D. 2000. *Astrophys. J.* 533:850
Schmelz JT, Baan WA, Haschick AD. 1987. *Astrophys. J.* 321:225
Schmelz JT, Baan WA, Haschick AD, Eder J. 1986. *Astron. J.* 92:1291
Schodel R, Ott T, Genzel R, Eckart A, Mouawad N, Alexander T. 2003. *Astrophys. J.* 596:1015
Smith HE, Lonsdale CJ, Lonsdale CJ, Diamond PJ. 1998. *Astrophys. J. Lett.* 493:L17
Snell RL, Howe JE, Ashby MLN, Bergin EA, Chin G, et al. 2000a. *Astrophys. J. Lett.* 539:L97
Snell RL, Howe JE, Asbhy MLN, Bergin EA, Chin G, et al. 2000b. *Astrophys. J. Lett.* 539:L101
Snell RL, Howe JE, Ashby MLN, Bergin EA, Chin G, et al. 2000c. *Astrophys. J. Lett.* 539:L93
Staveley-Smith L, Allen DA, Chapman JM, Norris RP, Whiteoak JB. 1989. *Nature* 337:625
Staveley-Smith L, Cohen RJ, Chapman JM, Pointon L, Unger SW. 1987. *Mon. Not. R. Astron. Soc.* 226:689
Staveley-Smith L, Norris RP, Chapman JM, Allen DA, Whiteoak JB, Roy AL. 1992. *Mon. Not. R. Astron. Soc.* 258:725
Strelnitskii VS. 1984. *Mon. Not. R. Astron. Soc.* 207:339
Tacconi LJ, Genzel R, Tecza M, Gallimore JF, Downes D, Scovilleo NZ. 1999. *Astrophys. J.* 524:732
Tarchi A, Henkel C, Chiaberge M, Menten KM. 2003. *Astron. Astrophys.* 407:L33

Tarchi A, Henkel C, Peck AB, Menten KM. 2002a. *Astron. Astrophys.* 385:1049
Tarchi A, Henkel C, Peck AB, Menten KM. 2002b. *Astron. Astrophys.* 389:L39
Taylor GB, Peck AB, Henkel C, Falcke H, Mundell CG, et al. 2002. *Astrophys. J.* 574:88
Teerikorpi P. 1997. *Annu. Rev. Astron. Astrophys.* 35:101
Townes CH, Schawlow AL. 1955. *Microwave Spectroscopy*. New York: McGraw-Hill
Townsend RHD, Ivison RJ, Smail I, Blain AW, Frayer DT. 2001. *Mon. Not. R. Astron. Soc.* 328:L17
Trotter AS, Greenhill LJ, Moran JM, Reid MJ, Irwin JA, Lo K. 1998. *Astrophys. J.* 495:740
Trotter AS, Moran JM, Greenhill LJ, Zheng X, Gwinn CR. 1997. *Astrophys. J. Letters* 485:L79
Ulvestad JS, Wrobel JM, Roy AL, Wilson AS, Falcke H, Krichbaum TP. 1999. *Astrophys. J. Lett.* 517:L81
Unger SW, Chapman JM, Cohen RJ, Hawarden TG, Mountain CM. 1986. *Mon. Not. R. Astron. Soc.* 220:1P
van Dishoeck EF. 2001. *ASP Conference Series* 231:244
van Loon JT, Zijlstra AA. 2001. *Astrophys. J. Lett.* 547:L61
Vermeulen RC, Ros E, Kellermann KI, Cohen MH, Zensus JA, van Langevelde HJ. 2003. *Astron. Astrophys.* 401:113
Walker RC, Matsakis DN, Garcia-Barreto JA. 1982. *Astrophys. J.* 255:128
Watson WD. 2002. *IAU Symp.* 206:464
Watson WD, Wallin BK. 1994. *Astrophys. J. Lett.* 432:L35
Wallin BK, Watson WD. 1997. *Astrophys. J.* 476:685
Wallin BK, Watson WD, Wyld HW. 1998. *Astrophys. J.* 495:774
Wallin BK, Watson WD, Wyld HW. 1999. *Astrophys. J.* 517:682
Weaver H, Williams DRW, Dieter NH, Lum WT. 1965. *Nature* 208:29
Weliachew L. 1971. *Astrophys. J. Lett.* 167:L47
Whiteoak JB, Gardner FF. 1973. *Astrophys. J. Lett.* 15:211
Whiteoak JB, Gardner FF. 1986. *Mon. Not. R. Astron. Soc.* 222:513
Whiteoak JB, Wellington KJ, Jauncey DL, Gardner FF, Forster JR, et al. 1983. *Mon. Not. R. Astron. Soc.* 205:275
Wilner DJ, Bourke TL, Ho PTP, Killeen NEB, Calabretta M. 1999. *Astron. J.* 117: 1139
Wilson WJ, Barrett AH. 1968. *Science* 161:778
Wilson AS, Braatz JA, Henkel C. 1995. *Astrophys. J. Lett.* 455:L127
Wilson AS, Shopbell PL, Simpson C, Storchi-Bergmann T, Barbosa FKB, Ward MJ. 2000. *Astron. J.* 120:1325
Wilson AS, Yang Y, Cecil G. 2001. *Astrophys. J.* 560:689
Wu CS, Lee LC. 1979. *Astrophys. J.* 230:621
Yamauchi A, Nakai N, Sato N, Diamond P. 2004. *Publ. Astron. Soc. Jpn.* 56:605

Annual Review of Astronomy and Astrophysics
Volume 43, 2005

CONTENTS